Sentinels4Carbon (Sense4Fire)

Sentinel-based fuel, fire and emissions products to constrain the changing role of vegetation fires in the global carbon cycle

ESA Contract Number: 4000134840/21/I-NB

Requirement Baseline Review Document (RBR)

6th December 2021, Version 1.1

Prepared by:

Matthias Forkel, Christine Wessollek, Christopher Marrs

Technische Universität Dresden, Faculty of Environmental Sciences, Dresden, Germany

Vincent Huijnen, Jos de Laat, Martin de Graaf

Royal Netherlands Meteorological Institute (KNMI), De Bilt, The Netherlands

Niels Andela, Alfred Awotwi

Cardiff University, School of Earth and Environmental Sciences, Cardiff, Wales, UK

Contents

1 Introduction

The purpose of the requirement baseline (RB) document is to provide a review, assessment and analysis of the main scientific challenges, knowledge gaps and scientific problems to be addressed in the Sense4Fire project. The RB will represent the basis for all the activities that will be carried out during the project. This document provides the following; a concise review of the state of the art and of the objectives (Chapter 1), identifies the candidate test areas (Chapter 2), provides a survey of datasets and methods to be used in development and validation including the associated risks (Chapter 3), consolidates the technical specifications of the target products (Chapter 4), and consolidates the science cases and scientific studies to be carried out (Chapter 5). Finally, the document provides an overview about related European and international projects and activities (Chapter 6) and defines the publication plan (Chapter 7).

1.1 State of the art

1.1.1 Quantifying the role of fires in the carbon cycle

Land ecosystems take up around 3.2 peta-grams carbon (PgC) per year which are around 30% of anthropogenic carbon dioxide (CO_2) emissions mainly from the burning of fossil fuels, cement production, and land use change (Quéré et al., 2018). The magnitude of the land carbon sink is further modified by the inter-annual variability in drought conditions, productivity, and fires (Poulter et al., 2014; van der Werf et al., 2004). Emissions from vegetation fires are estimated to vary between 1.8 and 3 PgC yr-1 (van der Werf et al., 2017), however studies that make use of high-resolution burned area maps from Sentinel-2 recently estimated up to 30-100% higher fire emissions in southern hemisphere Africa (Ramo et al., 2021). Fire emissions are rapidly changing in response to land use and climate. For example, a long-term decline in grassland and savannah burned area from land cover conversion and fragmentation has resulted in a 7% increase in land carbon uptake since the early 2000s (Andela et al., 2017) or a 19% increase since the 1960s (Arora and Melton, 2018). However, the recent climate driven extremes, like the record setting 2019 wildfires in Australia (Boer et al., 2020) or intensification of wildfires in California (Williamson et al., 2016) suggest the net contribution from fire may soon turn from sink to source. These concerns are further fuelled by the acceleration of Amazon deforestation (Barlow et al., 2020) and increasing distribution of understorey fires that could result in decreases in carbon storage several years after the fire (Aragão et al., 2018; Brando et al., 2020). Hence, fire-related emissions have a positive effect on radiative forcing and hence cause a warming effect on the atmosphere but aerosol emissions from fires also have a cooling effect (Kaufman et al., 2002; Ward et al., 2012).

The effect of fire on the climate system can be also assessed with global fire-enabled vegetation models that simulate the effect of humans, climate and vegetation on fire

occurrence, fire emissions and fire impacts on the carbon cycle (Hantson et al., 2016). However, the fire model inter-comparison project (FireMIP) has shown that these models do not sufficiently reproduce the temporal variability of fire occurrence (Hantson et al., 2020), do not reproduce observed relationships between fuel development and burned area (Forkel et al., 2019a) and show major uncertainties with respect to fire impacts on plant productivity and total ecosystem carbon storage (Lasslop et al., 2020). As a consequence, the overall role of fire emissions on the climate system is still uncertain (Lasslop et al., 2019).

Until now, knowledge about fire carbon emissions mostly relies on satellite observations of burned area that are combined with model simulations of biomass and combustion. Specifically, emissions (*E*) of a certain trace gas *x* during fire can be estimated from burned area (*BA*), available fuel loads (*FL*), the combustion completeness (*CC*) and trace gas species-dependent emission factors (*EF*) (Seiler and Crutzen, 1980):

$$E_x = BA * FL * CC * EF_x \quad (1)$$

This approach is for example used in the Global Fire Emission Database (GFED) to generate global datasets of fire emissions (van der Werf et al., 2006, 2017). GFED relies on a biogeochemical model to simulate vegetation biomass and litter fuel loads and approximates combustion completeness from modelled soil moisture. An alternative approach uses observations of fire radiative power (FRP) or fire radiative energy (FRE) as a proxy for fire emissions which is for example used in the Global Fire Assimilation System (GFAS) (Kaiser et al., 2012) and hence in the operational Copernicus Atmosphere Monitoring Service (CAMS). However, the GFAS approach calibrates the emission estimates against GFED and thus ultimately reliant upon the used assumptions of the biogeochemical model for fuel loads and combustion completeness. Information about emission factors are taken from laboratory, field, and aircraft measurements (Andreae, 2019; Andreae and Merlet, 2001). Parker et al. (2016) show pioneering work to use CH_4 and CO_2 satellite observations to constrain methane emission ratios. Combustion completeness can be estimated from field measurements of fuel loads before and after a fire (van Leeuwen et al., 2014). However, information on fuel loads, combustion completeness and emission factors is lacking at large scales which introduces major uncertainties in the quantification of fire emissions (Ichoku and Ellison, 2014). Moreover, coarse resolution estimates of burned area and active fire detections do not reveal the fire type, or aspects of fire behaviour related to smouldering and flaming combustion.

Carbon emissions from fires can also be constrained using satellite observations of atmospheric composition, in particular using carbon monoxide (CO) using various techniques, such as formal inversions (Hooghiemstra et al., 2011; Park et al., 2015), or mass budget analyses (Huijnen et al., 2016). Likewise aerosol and formaldehyde (HCHO) observations have been used as a proxy (Bauwens et al., 2016; Konovalov et al., 2014;

Petrenko et al., 2012). However, for any of these methods the estimated carbon emissions are not only subject to the aforementioned uncertainties on emission factors, but also to the dynamics of the emission process in the atmosphere and tracer lifetime.

1.1.2 State-of-the-art products on fuel properties

Several large-scale products are existing that can provide information on fuel loads or fuel moisture content (FMC). FMC can be estimated from various satellite technologies. For example, multi-spectral satellites have been frequently used to estimate the moisture content of living vegetation components (live-fuel moisture content, LFMC) (Chuvieco et al., 2002; Yebra et al., 2013; Quan et al., 2021) and the first operational LFMC products are now produced for e. g. Australia (Yebra et al., 2018). Also observations from microwave remote sensing have been shown to be valuable in estimating FMC. Early studies using data from the ERS-1 SAR and RADARSAT-1 satellites show significant correlations between radar backscatter and the duff moisture code, drought code and build-up index from the Canadian fire weather index system (Leblon et al., 2002; Abbott et al., 2007). Now Sentinel-1 C-band observation become increasingly used to estimate LFMC. . For example, Wang et al. (2019), coupled a bare soil backscatter model and the vegetation water cloud model in order to retrieve LFMC from Sentinel-1 dual-polarised backscatter observations. They obtained validation errors < 20% LFMC, which were lower than deriving LFMC from optical data using Landsat-8. Rao et al. (2020) combined Sentinel-1 backscatter and surface reflectance from Landsat-8 in a recurrent neural network to estimate LFMC. In their study, the integration of Sentinel-1 data significantly reduced the error in estimating LFMC. Some first studies compared derived products from passive microwave remote sensing with site measurements of LFMC. For example, vegetation optical depth (VOD) in X-band from AMSR-E showed medium to high correlation with LFMC at Mediterranean shrub sites which suggests that VOD could be used to estimate LFMC (Fan et al., 2018). The Sense4Fire consortium at TU Dresden is currently developing a methodology to estimate LFMC at large scales globally by using VOD retrievals from the VODCA dataset (Moesinger et al., 2020) and ground observations of LFMC from the Globe-LFMC database (Yebra et al., 2019) (VOD2LFMC approach, Figure 1). Thereby, we made a comparison of the relations between LFMC and VOD in Ku-, X- and C-band, which all show highly similar correlations with LFMC. However, as Ku-band observations offer the longest temporal coverage, we used Ku-band VOD to estimate LFMC. These various developments demonstrate that the estimation of fuel moisture content made good progress in the last years and those products can be potentially adopted in the estimation of fire emissions.

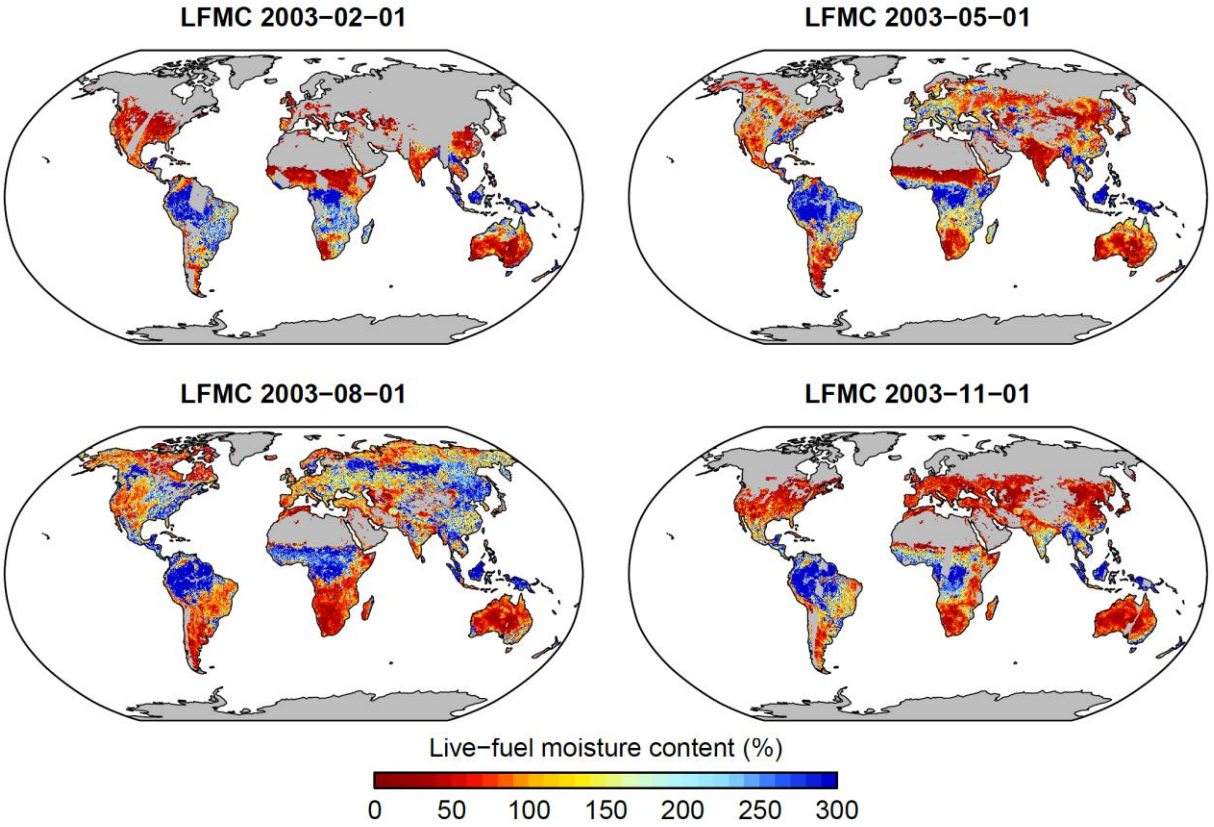

Figure 1: Example of large-scale patterns of LFMC and associated uncertainties as estimated from Ku-band VOD retrievals (VOD2LFMC approach) for four selected dates. The full dataset currently covers the years 2000 to 2017 and extensions are planned for the period 1987-2021. Grey areas are masked because of no vegetation cover or because VOD retrievals are not available during that day (Forkel et al. 2021, in preparation).

Estimates of fuel loads, i.e. the biomass content in various vegetation compartments and litter are less developed and have several limitations for the estimation of fire emissions. Only a few products have been specifically targeted to support the monitoring and modelling of fire and fire emissions. Fire-targeted products on fuel loads are for example the global fuelbed database (Pettinari and Chuvieco, 2016) and the North American Wildland Fuel Database (NAWFD) (Prichard et al., 2019). Both products combine land cover maps with representative values or statistical distributions of fuel properties such as biomass values for trees, shrubs, grass, woody debris and litter. The global fuelbed database combines the Globcover land cover map, maps of canopy height (Simard et al., 2011) and biomes to map fuelbeds and assigns fuel properties to each fuelbed value based mainly on the Fuel Characteristics Classification System (FCCS) (Ottmar et al., 2007; Pettinari and Chuvieco, 2016). The NAWFD specifically aims to quantify the uncertainty of fuel load estimates for different existing vegetation types. Therefore, statistical distributions of fuel loads based on field observations are assigned to each vegetation type in the NAWFD (Prichard et al., 2019). Although both databases are specifically defined for the purpose of fire modelling and quantifying fire emissions, their major

disadvantages are firstly that they do not provide information of the spatial variability of fuel loads within one vegetation type or fuelbed and secondly that they do not capture any temporal changes in fuel loads.

As an alternative, maps of above-ground biomass (AGB) from satellite retrievals could be used to quantify the spatial variability of fuel loads. Several maps of above-ground biomass became available in recent years for the tropics (Saatchi et al., 2011; Baccini et al., 2012; Avitabile et al., 2016), for northern ecosystems (Thurner et al., 2014), and globally (Santoro et al., 2021). Although these AGB maps provide information on the regional variability of biomass, they have a limited used for fire-related applications because they do not provide information on different fuel components such as biomass in canopies, wood, grass or litter and they do not provide information on the temporal dynamic of fuels.

Temporal dynamics of fuels can be approximated by a satellite-derived time series of vegetation indices or biophysical parameters. Retrievals of leaf area index (LAI), the fraction of absorbed photosynthetic active radiation (FAPAR) or of fractional cover of green vegetation (fCOVER) from multi-spectral sensors or of vegetation optical depth (VOD) from microwave sensors provide information on the temporal dynamics of vegetation. Specifically, VOD from L-band sensors such as SMOS is frequently used to estimate temporal changes in above-ground biomass (AGB) (Rodríguez-Fernández et al., 2018; Vittucci et al., 2019; Mialon et al., 2020). Additionally, VOD time series from sensors with shorter wavelengths (Ku, X and C-band) are representative of long-term changes in vegetation cover (Moesinger et al., 2020). However, the combined effetcs of various ecosystem properties such as biomass, water content and vegetation structure and cover on VOD are not yet fully understood and the complexity of the underlying relations are largely ignored in empirical relations between VOD and biomass (Zhang et al., 2021; Konings et al., 2021). Ideally, those factors should be taken account when using VOD observations as proxxies for changes in AGB. Several studies have demonstrated that time series of LAI, FAPAR and VOD are important predictors for the temporal dynamics of burned area (Forkel et al., 2017, 2019b; Knorr et al., 2014), whereby FAPAR has been proven to be best-performing predictor variable (Kuhn-Régnier et al., 2021).

Given the fact that products on the temporal dynamic and regional spatial variability of fuel loads for different fuel types do not exist yet, we aim to develop such products. Thereby we will combine the temporal information from LAI (or FAPAR) and VOD time series and the regional spatial information from AGB and land cover maps with the relevant thematic information on different fuel types from the North American Wildland fuel database and the fuelbed map by Pettinari and Chuvieco (2020).. As spatially and temporally dynamic fuel products do not exist yet, the scientific community has not yet defined any target accuracies or maximum errors for such products. Here we aim to

quantify uncertainties of fuel load estimates and to characterise errors by using various databases of ground observations. Databases of compiled ground observations on fuel loads are only available for a few countries (e.g. for the US in the NAWFD). We plan to propagate uncertainties from the NAWFD and characterise errors by using spatial cross-validation and model ensemble approaches. Other global databases on forest biomass (Schepaschenko et al., 2019), on allometry and allocation (Falster et al., 2015), or on litter loads (Holland et al., 2014) will also be used to calibrate and evaluate specific components of the approach to estimate fuel loads.

1.1.3 State-of-the-art products on fire dynamics

A range of global fire products exists, focused on quantifying burned area extent, fire behaviour, emissions, and operational response. Burned area products, like the MODIS based FireCCI51 (Lizundia-Loiola et al., 2020) and MCD64A1 collection 6 (Giglio et al., 2018) burned area datasets are among the most widely used fire products and form the basis for state of the art emissions datasets, such as GFED (van der Werf et al., 2017). Active fires in contrast, can be detected in near-real time and are therefore widely used to estimate near-real time emissions (e.g., GFAS; Kaiser et al., 2012). The GFED and GFAS datasets serve as the state of the art benchmarks for fire emissions. Active fire and FRP observations from the Visible Infrared Imaging Radiometer Suite (VIIRS) on board the NOAA20 and Suomi-NPP satellites provide mid-afternoon and night time fire detections (1:30 am/pm) and hence complement Sentinel-3 SLSTR observations (10 am/pm) to reconstruct the diurnal behaviour of fires. Information on fires is also provided in near-real time through the European Forest Fire Information System (EFFIS) and the Global Wildfire Information System (GWIS) of the Copernicus Emergency Management Service. Both systems provide detections of active fires based on the MODIS and VIIRS instruments, forecasts of fire weather and fire danger, and estimates of fire emissions from the CAMS system. Observations from the Sentinels are not yet included in these fire information systems. This shows the urgent need to explore the potential of Sentinel-3, Sentinel-5p, Sentinel-2 and Sentinel-1 to develop new integrated near-real time fire products of fire behaviour and emissions that can help to advance our understanding of and operational responses to fire emergencies.

Recently, several algorithms have been developed to track individual wildfires and their behaviour, a major step forward in our understanding of global fire occurrence and its drivers. The Global Fire Atlas is one of these datasets, and provides estimates of fire ignition points, sizes, speeds, expansion and duration derived from MODIS burned area maps (Andela et al., 2019). In this project, we will expand on these existing approaches to develop a system based on active fire detections to track individual wildfires, forming the basis of a new object-based emissions inventory that can be run in near-real time.

1.1.4 Potential of the Sentinels

The **Sentinels** provide several observations that can potentially be used in synergy to develop novel estimates of fire emissions and associated uncertainties:

- Sentinel-5p TROPOMI: The TROPOspheric Monitoring Instrument (Veefkind et al., 2012) provides observations on the absorbing aerosol index (AAI), aerosol layer height (ALH), nitrogen dioxide (NO2), carbon monoxide (CO) and formaldehyde (HCHO) (Landgraf et al., 2016; Torres et al., 2020).
- Sentinel-3 SLSTR: The Sea and Land Surface Temperature Radiometer allows the mapping of active fires and provides estimates of fire radiative power (FRP) (Weidong et al., 2020).
- Sentinel-3 OLCI: The Ocean and Land Colour Instrument allows the mapping of fire-induced land cover changes (e.g. burned area, fire severity) at medium resolution (300 m) (Lizundia-Loiola et al., 2021) and to retrieve pre- and post-fire vegetation properties such as FAPAR, LAI or fractional vegetation cover (fCOVER) (Fuster et al., 2020a).
- Sentinel-2 MSI: The Multispectral Instrument (MSI) allows the mapping of fire-induced land cover changes at a higher spatial resolution (10-20 m). A first burned area product is available for Africa (Roteta et al., 2019).
- Sentinel-2 MSI and Sentinel-3 OLCI are both sensitive to the water content of plant canopies and hence allow to estimate the life-fuel moisture content (Yebra et al., 2018) but a related product does not exist as yet.
- Sentinel-1 SAR: The C-band Synthetic Aperture Radar allows for the estimation of surface soil moisture (Bauer-Marschallinger et al., 2019) and can serve as a proxy for the moisture content of surface fuels (e.g. Rao et al. (2020))

Taken together, the Sentinels have a huge potential to observe and quantify fire dynamics in terms of pre-fire surface conditions (vegetation cover and fuel moisture content), fire behaviour (FRP, burned area, fire size) and fire effects on the atmosphere (fire emissions of trace gases and aerosols). However, thus far this combined potential has not been exploited.

1.2 Aims and objectives

The aim of this activity is to increase the scientific understanding of fire dynamics and their role in the carbon cycle by integrating observations from the Sentinels into new Earth observation products. We understand fire dynamics as all processes that contribute to pre-fire conditions of the land surface (i.e. fuel loads and fuel moisture), fire behaviour (fire ignitions, spread, speed, size, burned area, thermal emissions and radiative power), combustion and production of fire emissions (combustion completeness, biomass burning, composition of emissions) and the effect of fire emissions on atmospheric

composition (injection height, smoke plumes, atmospheric gas composition, aerosols). This aim will be addressed within the duration of this activity by two specific objectives:

Objective 1: Develop and generate for the three regions of interest novel and advanced geo-information products to quantify the spatial-temporal variability in fuel conditions, fire behaviour and fire emission estimates mainly based on observations from Sentinel-3 and -5p and supported by data from Sentinel-1 and -2 and additional European Earth observation datasets.

Objective 2: Demonstrate the value of the novel products in coordination with early adopters to increase the scientific understanding of fires by assessing three science questions related to (1) the effects of fuel dynamics on fire behaviour, (2) the effects of fire behaviour on short- and long-term fire emissions, and (3) the role of uncertainties in estimating fire emissions.

Within Objective 1, we will develop and generate novel products to quantify the spatial-temporal variability in fuel conditions, fire behaviour and fire emission estimates:

- Vegetation fuel loads and combustion completeness will be estimated using a novel fuel data integration framework that combines (1) surface reflectance and vegetation information from Sentinel-3, Sentinel-2 and Proba-V; (2) land cover and above-ground biomass from the ESA Climate Change Initiative and from the Copernicus Land Service; (3) vegetation optical depth from SMOS and the VODCA dataset; and soil moisture from Sentinel-1 and Metop/ASCAT.
- Fire behaviour and burned area will be quantified using novel mapping of individual fires based on thermal anomalies and the diurnal fire cycle from Sentinel-3 and of burned area estimates from Sentinel-2. We will combine these data with Sentinel-based fuel information to identify fire types and to estimate fire emissions from a bottom-up approach.
- Fire effects on atmospheric composition will be quantified by contrasting observations of trace gases (CO, NO_2, formaldehyde) and aerosols from Sentinel-5p with model results from the Copernicus Atmosphere Monitoring Service (CAMS) modelling system. These observations will help to constrain combustion completeness and to estimate dynamic emission factors and to quantify fire emissions from a top-down approach.

Within Objective 2, we will address the following three scientific questions to increase the scientific understanding and modelling of fire dynamics:

- (Q1) How do changes in land ecosystems affect fuel loads and fuel moisture and hence fire behaviour?
- (Q2) How do fires contribute to short- and long-term carbon emissions?

- (Q3) To what extent three key uncertainties (emission factor, injection parameterisation and tracer lifetime) affect the top-down estimates on total carbon emissions released by fires?

2 Test areas

2.1 Overview and selection

Based on initial data analysis we have identified four test areas within the three larger study regions that include a range of representative land cover and fire types (Figure. 2). These regions include a transect from frequently burning tropical forests to savannah in Brazil, an area with small agricultural and large savannah fires in southern hemisphere Africa, and two regions in the Russian Federation (Figure. 3). For Russia, we explicitly selected two regions to cover the full range of regional climates, vegetation, and fire types, including tundra, forest, agricultural and steppe fires. For a preliminary analysis we have for each region identified the fire season during 2020 for atmospheric modelling purposes. Fire activity can vary considerably from year-to-year and 2020 was found to be of particular interest for the selected regions (e.g., extensive drought driven understorey fires in Brazil, and large forest fires in Eastern Russia).

Figure 2: Location of the test areas for the development of methods

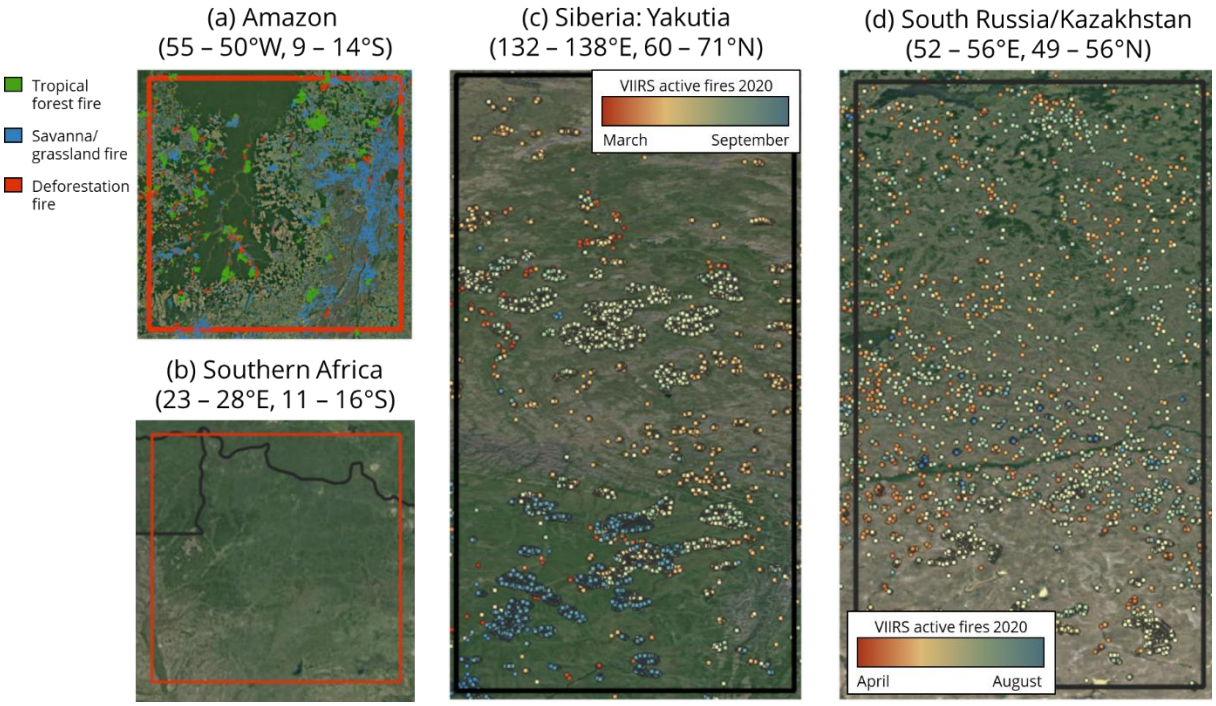

Figure 3: Detailed maps of the test areas. In the Amazon region in (a) fire types are mapped based on VIIRS active fire observations using a recently developed approach by N. Andela. In (c) and (d) active fires in 2020 are mapped from VIIRS observations. No active fires are shown in the southern Africa test site (b) because a large proportion of this landscape is burned annually resulting in a large amount of active fire detections which cannot be interpreted at this scale.

2.2 Brazil

Decades of expansion of the land use frontier into tropical forests are increasing concerns about Amazon forest conservation. However, until recently the role of fire in the process of tropical forest degradation remained unclear because satellites can detect fires, but not their type and underlying causes. Our selected study region (Figure. 3a), including the Xingu protected areas, includes a mix of fire types relevant for forest degradation. First, the region includes large areas of active deforestation, followed by fires to remove residual organic material and prepare fields for agriculture or grazing. Second, it is a region that is particularly sensitive to forest fires during drought years, such as 2020. Finally, the region includes extensive and frequently burning natural savannah, the third important regional fire type. Initial results indicate good capability to separate these regional fire types (Fig. 3a).

2.3 Southern Africa (Angola, DRC, Zambia)

The second study region in southern hemisphere Africa represents a large moisture gradient, from more arid savannahs to dense woodlands (Figure. 3b). Therefore, this region includes both large grassland fires and woodland degradation fires towards the end of the dry season. In addition, the region also highlights the strong human signature

on fire occurrence, including many small agricultural burns and higher intensity burns associated with land clearing. Identifying these different fire types and their temporal contributions to burned area and fuel consumption will enable us to use top-down emissions modelling to constrain emissions factors, combustion efficiency and total carbon emissions.

2.4 Siberia/Yakutia

The third region covers an environmental gradient ranging from open Tundra landscapes in the north, towards increasingly dense Taiga forests in the south (Fig. 3c). Fuel loads and properties such as drainage conditions and tree species composition are important controls on fire emissions in boreal forests (Walker et al., 2020). Recently, there has been an increased interest in tundra burning because of subsequent acceleration of permafrost melt and subsequent increase in shrubs and trees. In contrast, regional warming has intensified burning of Taiga forests, with unknown outcomes for forest density, carbon storage and post-fire recruitment and recovery (Barrett et al., 2020; Shvetsov et al., 2019). Here we aim to separate crown from ground fires, to better understand wildfire emissions and the long-term consequence for above ground biomass. Our study will be the first to identify these regionally important fire types and constrain their emissions and therefore presents an important step forward in our understanding of ecosystem change.

2.5 Southern Russia/Kazakhstan

The fourth study region includes more arid northern ecosystems, along a moisture gradient from Steppe to Taiga (Fig. 3d). In this particular region, the more productive lands have been converted into extensive croplands (mainly various types of cereals), and crop residue burning is common practice. In contrast, the southern part presents more arid steppe grasslands, where large and rapidly moving low-intensity fires are frequent. Our approach will help to quantify agricultural burning and emissions across the region and provide new insights into changing patterns of fire occurrence across the Asian Steppe, an ecosystem that has seen rapid decline in fire activity over the past decades.

3 Data and methods

3.1 Vegetation and fuel properties

3.1.1 Datasets to estimate fuel loads

Further information on the used datasets can be found in the Database Description document. In order to estimate the spatial and temporal variability in fuel loads and associated uncertainties, we will use the following datasets:

- FAPAR, LAI and fCOVER from Sentinel-3 OLCI and Proba-V, Version 1.1. (Fuster et al., 2020b).
- Above-ground biomass from the Biomass_cci project V2 for 2017 (Santoro et al., 2021).
- Forest canopy height from a dataset that combines GEDI height estimates with Landsat observations for the year 2019 (Potapov et al., 2021).
- Land cover from the Land cover_CCI project V2.0.7 for the period 1992-2015 and from the Copernicus Climate Change Service for 2016-2020
- VOD from the VODCA dataset V1 in Ku-, X- and C-bands (Moesinger et al., 2020) and in L-band from SMOS using retrievals from LPRM retrieval (van der Schalie et al., 2017).
- Fuel load measurements and derived statistics for different vegetation types from the North American Wildland Fuel database (NAWFD) (Prichard et al., 2019) and from the global fuelbed map (Pettinari and Chuvieco, 2016)
- Measurements of tree height and estimates of AGB or biomass in tree stems, branches and leaves from the Biomass And Allometry Database (BAAD) (Falster et al., 2015) and the Forest observation system (Schepaschenko et al., 2019).

FAPAR, LAI and fCOVER retrievals from Proba-V and Sentinel-3 are available at 300 m spatial resolution and 10-daily temporal resolution for the period since January 2014 from the Copernicus Global Land Service. The datasets come with uncertainty estimates and various quality flags. Validation results have shown a higher performance of the Proba-V FAPAR/LAI/fCOVER products in comparison with ground observations than corresponding retrievals from MODIS (Fuster et al., 2020a). Although both the Proba-V and Sentinel-3 product should be very consistent as consistency was enforced during the development of those products, we will still carefully assess the consistency between the estimates from the two sensors and apply for example CDF matching if needed. The FAPAR, LAI and fCOVER products will be used as input into the approach to estimate the temporal dynamic of canopy and herbaceous fuel loads and fuel moisture.

AGB from Biomass_cci is available at 100 m spatial resolution for the years 2010, 2017 and 2018. The dataset provides the total AGB of all woody components (stem, bark, branches, and twigs) of trees and comes with an estimate of uncertainty. The AGB maps from the different years should not be used to calculate any temporal changes in AGB. We will use the AGB from a single year as input to our methodology to estimate fuel loads by providing a constraint on the total woody AGB.

The map of forest canopy height from Potapov et al. (2021) combines estimates of canopy height from the GEDI space-borne Lidar with observations from Landsat to produce a global map of forest canopy height at 30 m spatial resolution. The dataset is a major advancement over the long-lasting state-of-the-art dataset by Simard et al. (2011). We will

use the GEDI/Landsat-based dataset as a constraint on tree height in order to estimate above-ground biomass in different tree compartments (stems, branches, leaves) in an allometry model.

Land cover maps from the CCI provide annual maps of the distribution of land cover classes for the years 1992 to 2015 at 300 m spatial resolution. Land cover maps from the Copernicus Climate Change Service use the same classification as the CCI maps and extend the dataset for the years 2016 to 2020. The maps were developed to be used for assessments of land cover change. The maps will be used as input to estimate fuel loads by providing information on the fractional cover of herbaceous vegetation and trees and tree types. The maps will be also used to mask water bodies and wetlands (Lamarche et al., 2017).

The VODCA dataset provides harmonised time series of VOD in Ku-, X- and C-bands at 0.25° spatial resolution for the period 1987-2017, 1997-2018, and 2002-2018, respectively (Moesinger et al., 2020). The dataset will be used to constrain parameters of our approach with respect to the temporal dynamics in fuel moisture and biomass at large scales. Additionally, the usability of VOD in L-band from SMOS will be assessed. While L-band VOD from the SMOS-IC retrieval algorithm has been widely used to estimate changes in AGB (Wigneron et al., 2021), we will here use SMOS retrievals using the LPRM algorithm (van der Schalie et al., 2017), which is the same radiative transfer model used for the VODs in the VODCA dataset. L-band VOD has a higher penetration depth in the canopy than C-, X- or Ku-band VOD. Hence, L-band VOD can be used as proxy for woody fuel loads and moisture (Di Giuseppe et al., 2021) and C-, X- or Ku-band VOD can be used as proxies for canopy fuel loads and moisture (Frappart et al., 2020). The VOD datasets can provide a coarse-resolution constraint on regional changes in AGB and LFMC.

The NAWFD provides a map of existing vegetation types for the United States and for each vegetation type associated measurements and statistical distributions of fuel loads for different fuel types such as trees, shrubs, herbaceous vegetation, fine and coarse woody debris, litter and duff. These fuel classes are for some vegetation types further differentiated into different size classes (e.g. 1, 10 and 100 hour fine woody debris) (Prichard et al., 2019). The dataset will be used as reference to develop machine learning models to estimate surface fuels with associated uncertainties. Additionally, the global fuelbed map from Pettinari and Chuvieco (2016) will be used to compare our estimates of surface fuels with an alternative product.

The BAAD provides field and greenhouse measurements of tree allometry (e.g. tree height, DBH) and biomass in tree components such as leaves, branches, and stems for various tree species and functional groups (Falster et al., 2015). This information will be used to calibrate allometric models between tree height, AGB and biomass in stems, branches and leaves in order to estimate fuel loads for different tree components.

Although BAAD and NAWFD do not spatially overlap, both databases are complementary in terms of information content because BAAD provides biomass estimates for different tree compartments and NAWFD provides biomass estimates for trees (but not compartments), shrubs herbaceous vegetation and surface fuels.

The Forest Observation System provides measurements of tree height and associated estimates of AGB for various field sites around the globe (Schepaschenko et al., 2019). The dataset can complement information from BAAD will be used to evaluate our estimates of tree fuel loads.

3.1.2 Datasets to estimate fuel moisture

In order to estimate the spatial and temporal variability of fuel moisture, we will use the following datasets:

- Surface reflectances from the Sentinel-3 OLCI and SLSTR L2 Synergy product
- LFMC estimates from the VOD2LFMC approach (Forkel et al. 2021, in preparation)
- LFMC retrievals from MODIS (Yebra et al., 2018)
- LFMC measurements from the Globe-LFMC database (Yebra et al., 2019)
- Soil Water Index (SWI) from Metop-ASCAT
- Sentinel-1 backscatter

Surface reflectance along the red edge and in the near (NIR) and short-wave infrared (SWIR) from multi-spectral instruments are sensitive to LFMC (Yebra et al., 2013). Hence, we propose to use the Sentinel-3 OLCI/SLSTR synergy product, which covers the NIR (OLCI bands) and SWIR (SLSTR S6), and are provided at a common grid. However, the development of a new LFMC product from Sentinel-3 OLCI observation is likely beyond the scope of Sense4Fire and such developments are currently executed in other projects (Chapter 6). Hence, we propose to compute various spectral indices that make use of differences between the red bands, NIR and SWIR and that are sensitive to water stress (Yebra et al., 2013). For example, the Normalised Difference Infrared Index (NDII) can be adapted to the Sentinel-3 SYN observations and will be explored as a proxy for LFMC. These spectral indices will be compared with LFMC measurements from the Globe-LFMC database and with estimates from the VOD2LFMC approach and from MODIS and will be used as proxies for LFMC.

The SWI from Metop-ASCAT is available at 0.1° spatial resolution since 2007. SWI will be used as proxy for dead fuel moisture content. Additionally, backscatter observations from Sentinel-1 will be used as proxy for dead fuel moisture content at a higher spatial resolution in selected case study sites.

3.1.3 Estimating and validating fuel loads

The estimation of fuel loads will be based on two different approaches.

The *first* approach will be based on an **empirical allometry model** that estimates the fuel loads of different biomass compartments of trees and herbaceous vegetation by using total AGB (or alternatively canopy height) and FAPAR or LAI as input. The biomass of stems (BM_{stem}), branches ($BM_{branches}$), leaves (BM_{leaf}), total woody biomass (BM_{wood}) and total AGB will be estimated from total AGB (or canopy height) using allometric relations:

$$\mathrm{BM_{stem}} = \mathrm{a1} \times (\mathrm{height})^{\frac{1}{\mathrm{a2}}} \quad (2)$$

$$\mathrm{BM_{branches}} = \mathrm{a3} \times (\mathrm{BM_{stem}})^{\frac{1}{\mathrm{a4}}} \quad (3)$$

$$\mathrm{BM_{leaf}} = \mathrm{a5} \times (\mathrm{BM_{stem}})^{\frac{1}{\mathrm{a6}}} \times \mathrm{P} \quad (4)$$

$$\mathrm{BM_{wood}} = \mathrm{BM_{stem}} + \mathrm{BM_{branches}} \quad (5)$$

$$\mathrm{AGB} = \mathrm{BM_{wood}} + \mathrm{BM_{leaf}} \quad (6)$$

$$\mathrm{BM_{herb}} = \frac{\mathrm{LAI_{herb}}}{\mathrm{SLA}} \quad (7)$$

Whereby *a1* to *a6* are the parameters of the allometric equations. The equations follow the approach used in Thurner et al. (2014) to estimate tree biomass compartments from satellite retrievals of growing stock volume. The index *P* in equation 4 is the phenological status of the canopy and ranges between 0 (no leaves) and 1 (full leaf cover). *P* will be taken from the seasonal dynamic of fCOVER. SLA is the specific leaf area (leaf area per mass of carbon) and will be used to compute the biomass of herbaceous vegetation. The allometric parameters will be estimated from the Biomass And Allometry Database and initial results demonstrate that this model can represent observed biomass compartments (Figure 4). The model can use either canopy height or total AGB as input. Temporal changes in these biomass components will be estimated by applying the empirical allometric model to the time series of either AGB or canopy height. AGB time series will soon become available from the ESA-funded BIOMASCAT project. Alternatively, annual changes in canopy height will be estimated using a space-for-time substitution approach by calculating a regression between spatial maps of canopy height from the GEDI/Landsat dataset and by using LAI, land cover and VOD as predictor variables. Uncertainties in the final estimates of tree biomass compartments will be estimated by propagating uncertainties in model parameters (i.e. parameters *a1* to *a6* and parameters of the spatial regression to estimate temporal changes in canopy height). The model will be calibrated for each test area against AGB and canopy heights maps by accounting for the uncertainty of those dataset and of the model parameters in a joint cost function.

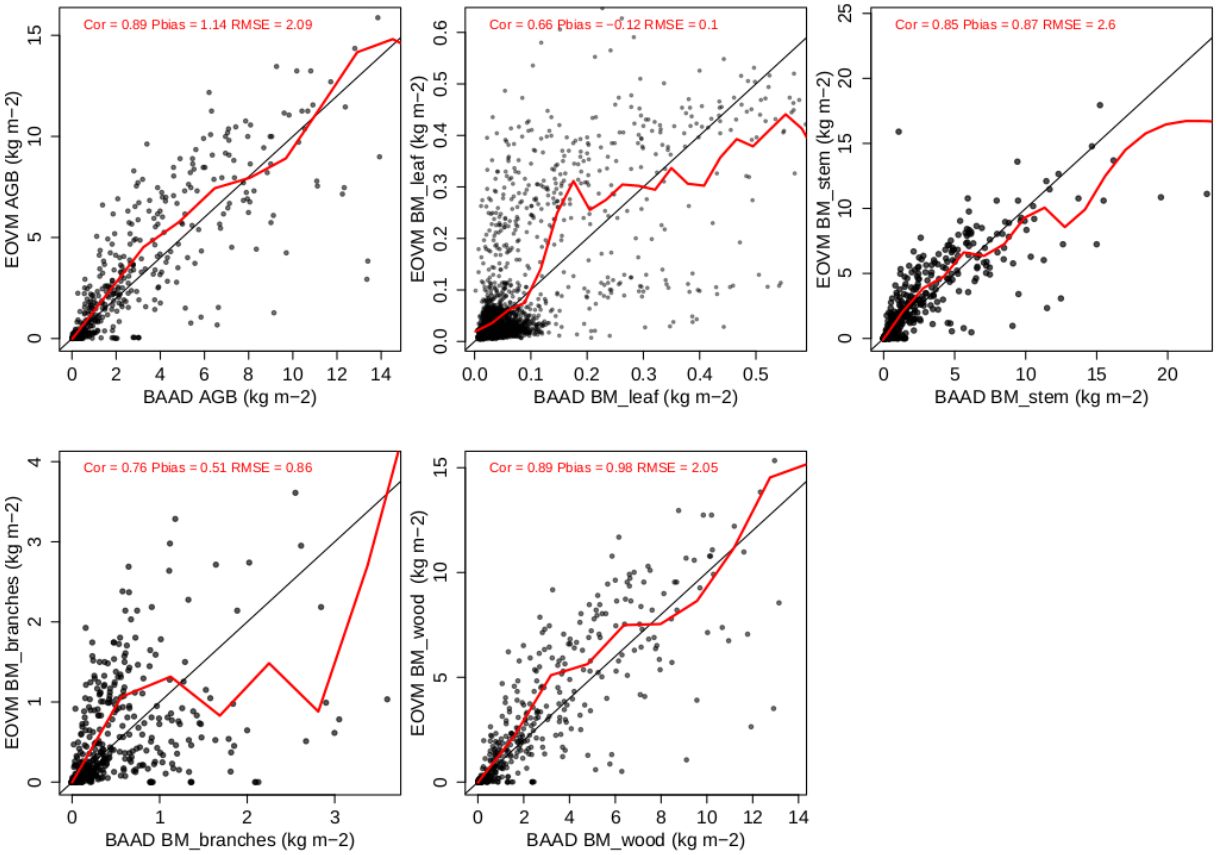

Figure 4: Results of the calibration of the parameters a1 to a6 from the empirical allometric model (denoted as EOVM) against measurements of different biomass compartments from BAAD. The red curves are smoothing splines fitted to the scatter and represent under- and overestimation.

The *second* approach to estimate fuel loads will be based on **machine learning** to transfer the measurements from the NAWFD database to other regions. Therefore, a set of grid cells will be sampled from each existing vegetation type in NAWFD fuelbed map and the corresponding land coverages (ESA CCI and C3S), LAI (Proba-V/Sentinel-3) and AGB (ESA CCI) values will be extracted from the Earth observation datasets. These values will be then used as predictors to estimate the statistical distributions of fuel loads as included for each vegetation type in the NAWFD. By taking different samples of grid cells and different samples of fuel load values from the NAWFD, we will generate an ensemble of machine learning models. This ensemble will be used to predict the statistical distribution and uncertainty of fuel load estimates. Spatial cross-validation will be used to assess the performance of each ensemble member. The trained machine-learning model ensemble will be then applied to the test areas by using the observations of LAI, land cover and AGB as input. In order to further assess the robustness of this approach, we will quantify how well the NAWFD database captures the ecological feature space in the test areas.

3.1.4 Estimating combustion completeness and fuel consumption

Fuel consumption (FC) and combustion completeness (CC) can be estimated using various approaches. The *first* approach follows the approach by Seiler and Crutzen (1980) that is also used in GFED (van der Werf et al., 2017) and computes FC as a function of fuel loads (FL) and CC:

$$\mathrm{FC} = \mathrm{FL} \times \mathrm{CC} \quad (8)$$

Thereby CC is estimated by linearly scaling modelled soil moisture to the range [0-1], which indicates no or complete combustion (van der Werf et al., 2017). This approach can be adopted by using a scalar dependent on the satellite-derived estimates of SWI and LFMC in order to compute CC.

In a *second* approach, CC can be computed by combining fire radiative energy (FRE) with burned area (BA) and fuel loads. Following the approach used in GFAS (Kaiser et al., 2012), the burned dry matter (DM_b) is directly related to FRE as:

$$\mathrm{DM_b} = \mathrm{FRE} \times \mathrm{cf} \quad (9)$$

whereby *cf* is a conversion to convert the emitted energy release of the fire (unit: MJ) into burned dry matter (unit: kg). Based on a first empirical study this conversion factor was estimated as *cf* = 0.368 kg/MJ (Wooster et al., 2005). Another study reported a range between 0.23 to 0.77 kg/MJ for different burning experiments or a general slope of 0.453 kg/MJ of the linear regression between combusted fuel and FRE (Freeborn et al., 2008). For the application in GFAS, conversion factors were estimated from simulations of burned dry matter from GFED and range between 0.13 kg/MJ (agriculture with organic soil), 0.96 (topical forests), 1.55 (extratropical forests) up to 5.87 (peat) (Kaiser et al., 2012). Burned dry matter is related to fuel consumption as:

$$\mathrm{DM_b} = \mathrm{FC} \times \mathrm{BA} = \mathrm{FL} \times \mathrm{BA} \times \mathrm{CC} \quad (10)$$

By combining equations 9 and 10, CC can be computed as:

$$\mathrm{CC} = \frac{FRE \times cf}{FL \times BA} \quad (11)$$

The disadvantage of this approach is that the uncertainty and the spatial-temporal variability of the *cf* parameter is unknown and the approach does not make use of any information about fuel moisture conditions that surely affect the combustion process.

A *third* approach combines the first two approaches. Therefore, CC can be estimated using an inverse approach by inverting a simple model of FRE against observed FRE. Based on equations 9 and 10 FRE can be simulated as:

$$\mathrm{FRE_{sim}} = \frac{BA \times CC \times FL}{cf} \quad (12)$$

with CC being a scaling function of fuel moisture (CC = f(SWI) or CC = f(LFMC)). Based on known burned area and the estimated fuel loads, the parameters of the scaling function for CC and the parameter *cf* can be estimated by calibrating the simulated FRE against observed FRE in a Bayesian framework. As a result, this approach would yield estimates of CC and FL with associated uncertainties by using most of the available datasets.

Alternatively, CC could be also constrained from direct mapping of changes in surface reflectance during a fire. For example, Roy et al. (2019) use spectral observations from Landsat and Sentinel-2 before and after a fire to estimate a parameter fCC (fCC = f * CC) that is the product of the fraction of the pixel that burned (f) and combustion completeness (CC):

$$\Delta\rho_\lambda = \left(\rho_\lambda^U - \rho_\lambda^B\right) \times \mathrm{fCC} \qquad (13)$$

Where ρ^U and ρ^B are the reflectance of the unburned and burned pixel in a certain spectral band with wavelength λ. As the product fCC is directly related to the product of BAxCC in equation 12, the combination of equations 12 and 13 would allow to constrain combustion completeness and hence fuel consumption by a) observations of FRE (from Sentinel-3) and b) observations of changes in surface reflectance from either Sentinel-3 or Sentinel-2.

Another potential alternative approach to estimate fuel consumption can be only applied to live fuels (leaves, grass). Examples from the Copernicus Global Land Service demonstrate that temporal changes in Porba-V/Sentinel-3 LAI, FAPAR and fCOVER can be associated to fire events. Hence observed declines in LAI, FAPAR, fCOVER during or shortly after a fire event will translate into a loss of carbon in the allometry model and could be directly taken as estimates of the consumption of live fuels. However, this approach is subject to errors and uncertainties in the estimated fuel loads. The feasibility of this approach can be only assessed once we obtain knowledge on the errors and uncertainties of the fuel load estimates from the empirical allometry model and ideally, errors from the used LAI, FAPAR and fCOVER datasets would need to be propagated. We plan to test and compare the applicability and results all of these approaches for a sample of individual fire events within the four study regions. This comparison will guide the final decision for one approach.

All of these three approaches can be further constrained by using a field measurement database of *CC* and *FC* (van Leeuwen et al., 2014). Although this database is spatially sparse, it at least allows us to obtain statistical distributions of fuel consumption.

3.1.5 Risks and solutions

We identify the following risks for the development of fuel and bottom-up fuel consumption products:

- Gaps and noise in satellite observations, specifically in FAPAR/LAI/fCOVER and surface reflectance, e.g. due to clouds
- Inconsistencies between the different Earth observation products, including the assumptions in the used retrieval algorithms and the applied ancillary data.
- Representativeness of the fuel and biomass data bases for the study regions
- Insufficient process understanding and model structures

Gaps and noise in satellite observations because of atmospheric distortions or clouds could cause estimation of unreliable temporal dynamics in estimated fuel loads and moisture. The risk is probably rather small for the Proba-V/Sentinel-3 FAPAR/LAI/fCOVER data because gap filling and smoothing algorithms were already included in the production of this data. However, we might apply additional time series smoothing and gap-filling algorithms if needed. Alternatively, monthly composites will help to reduce any effects of missing values and/or noise. The smoothed time series will be interpolated to daily time steps in order to allow estimations of fuel loads in the case of missing observations. Any longer gaps that permanently occur during a season (e.g. during the winter months in northern ecosystems) will be filled with the observed minimum value from all years of observations which is representative of the leaf cover of evergreen species during winter (Beck et al., 2006; Forkel et al., 2015).

Inconsistencies might be present between the AGB, canopy height, land cover and FAPAR/LAI/fCOVER datasets on the one hand and between FRE and BA datasets on the other hand because they have been partly derived from different sensors with different overpass times, spatial resolutions and using different ancillary datasets. For example, the Sentinel-3 OLCI FAPAR dataset assume no orographic effects and a horizontally homogenous structure of each pixel which might result in inconsistencies if the land cover maps indicated e.g. mixed forests. The CCI biomass dataset makes additional use of the CCI land cover maps to delineate forested areas and hence these two datasets should be consistent. However, the CCI biomass dataset and the GEDI/Landsat canopy height dataset were produced completely independent with using different input datasets. Hence, there might be pixels in which one dataset shows for example high biomass and the other low canopy height. Therefore the datasets will be screened for unlikely combinations of AGB, canopy height and land cover and such affected pixels will be flagged and potentially masked. We will use the land cover data to mask in all datasets areas that are covered by water, wetlands or bare soils. The estimates of live fuel loads will try to achieve consistency with all datasets by finding an optimum AGB and canopy height and by considering the uncertainty of these datasets. Specifically, the uncertainty of each product will be considered as priors in a cost function to derive optimal estimates of fuel loads.

The NAWFD and BAAD databases do spatially not coincide with the location of our selected test areas and hence the information in those databases might not be representative enough for the vegetation types and ecosystem properties in the test sites. However, the NAWFD database covers various ecosystems from the Alaskan Tundra, to temperate forests, tropical forests in Florida and semi-arid ecosystems in the south-western US. We will investigate the multi-variate feature space of vegetation properties covered by the NAWFD and by the test areas and will quantify the distance to the feature space of the reference data. This information will help to rate the confidence in the estimated fuel properties.

The proposed empirical and machine learning models reflect our current knowledge might be insufficient to capture realistic patterns of biomass compartments or dead fuel loads. In order to diagnose any insufficiencies of the models, we will perform an analysis of model residuals in comparison to the reference data. This analysis will help to identify missing processes or predictors that can be then included during later phases of model development.

3.2 Fire behaviour and types

Traditional emissions inventories are based on a combination of burned area and modelling (e.g. GFED), or active fire detections calibrated against bottom up or top-down constraints of emissions (GFAS, QFED). One of the key limitations of such gridded approaches is the lack of understanding of the underlying processes and fuel types burning. Accurate separation of different fire types is important because they are directly related to the model parameters (e.g. combustion completeness, conversion factors, emissions factors). Here we propose a highly novel object-based approach for fire characterisation. We will combine the morning (10 am) and evening (10 pm) overpasses from SLSTR with mid-afternoon (1:30 pm) and night-time (1:30 am) overpasses from VIIRS to track individual wildfires as they evolve. Andela et al. (under review) have piloted this approach based on active fire detections from the VIIRS instruments on-board NOAA-20 and Suomi-NPP and found that they could accurately identify various fire types across the Amazon basin in near-real time. Nevertheless, estimates of corresponding burned areas and emissions remained uncertain, particularly for small fires or fast moving grassland fires.

3.2.1 Tracking fire objects

Following the existing approaches developed by Andela et al. (2019), we will derive an active fire based dataset of individual wildfires and their behaviour for the three study regions over the period 2019 - 2023. Here we will expand on this approach by including Sentinel-3 SLSTR active fire detections in the algorithm to provide more complete coverage of areas burned by fast-moving savannah fires, and to further expand the

detection of small short-duration fires during the morning. In addition, we will explore regional optimisation of certain model parameters. For example, a cut-off value defining how long a fire can take to spread from one grid cell into the next, is used to separate adjacent fires burning at different times in the season. We will introduce short cut-off values for cropland areas and longer values for high fuel systems (building on Andela et al., 2019). For open cover types, fires can become too fragmented based on fire spread rates of multiple kilometres per day, for those instances we will introduce another parameter to merge proximate but disconnected clusters of active fire detections into single fire events. Our approach will be based on developing a database of reference fires based on visual interpretation of active fires and Sentinel-2 burned area and subsequent optimisation of the model parameters for different fire and fuel types.

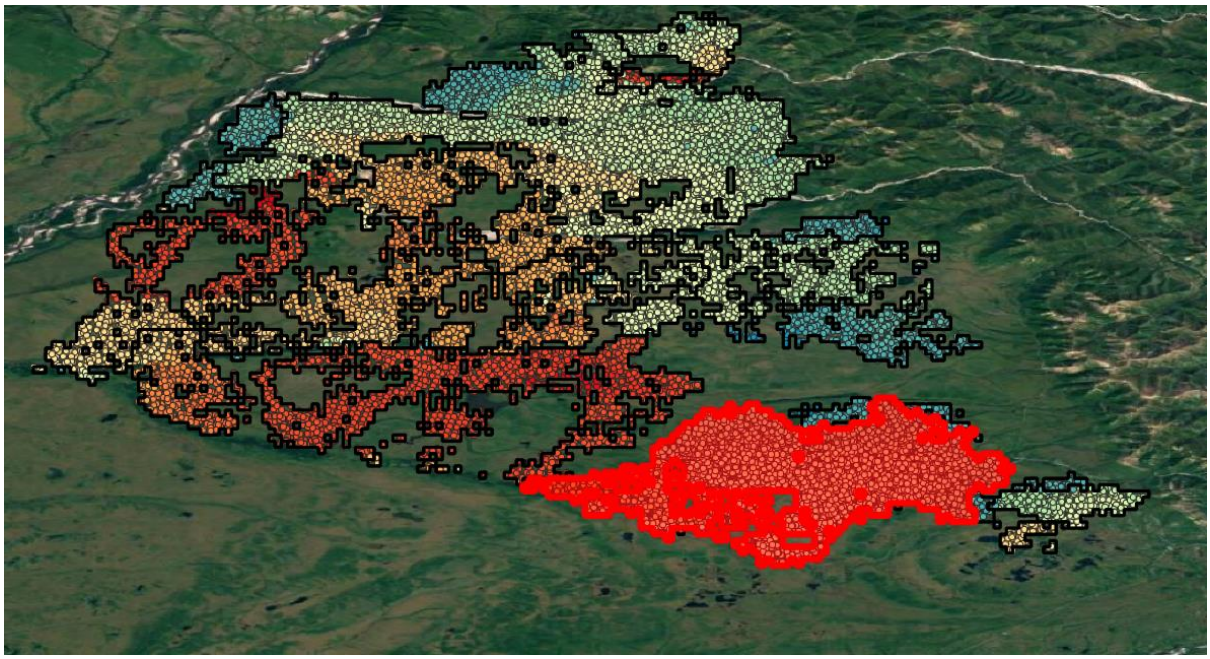

Figure 5: Initial results of the algorithm for a large cluster of wildfires burning in the Russian Taiga study region. For this cluster, the first active fire pixels were detected during late June 2020 (red) and fires burned until the end of August (blue). The figure highlights how these large fires often include multiple ignition locations. Nevertheless, the selected fire (red polygon) also shows further optimisation of the parameters would be helpful to identify the precise fire extent. The point cloud of active fire detections is dense in forested landscapes but may not capture the full extent of burned area in open cover types.

3.2.2 Burned area estimates

We will investigate regional relationships between fire perimeters from our active fire based approach and burned area estimates from Sentinel-2. Based on the Amazon pilot study and previous literature (Oliva and Schroeder, 2015; Veraverbeke et al., 2014), we expect good correspondence between fire perimeters and burned area for fires in forested cover types. Early results of our algorithm highlight an exceptional performance for tropical forests understorey fires that are often hard to detect based on changes in

surface reflectance alone (Fig. 6). We expect that in particularly the night-time detections of SLSTR will provide additional evidence of understorey fire location. Fires are typically still active at 10 pm, but smaller differences in brightness temperatures can be detected under night-time conditions, increasing the algorithm sensitivity to low-intensity fires. For fast moving fires in low fuel load open cover types and small fires, we will derive regional scaling factors to translate detected area by active fires to regional burned area estimates. This is similar to existing emissions inventories, for example the small fire burned area estimates from GFED4s (Ward et al., 2012; van der Werf et al., 2017). The new GFED5s burned area product (under development) relies on MCD64A1 col 6 burned area and compares these estimates to existing regional Landsat and Sentinel-2 burned area products for different bins of tree cover to provide additional estimates of small fire burned area. In comparison, our product will primarily rely on the burned area from the gridded active fire detections (fire perimeters) and provide fire-type specific scaling factors for fast-moving and small fires by scaling against regional estimates of burned area from Sentinel-2.

We expect that the relationships between burned area and individual fire perimeters or detections will vary regionally. For example, small fire burned areas will vary with the size of agricultural fields and regional distribution of crop types. Similarly, the extent to which burned area can be mapped directly by the active fire perimeters will depend on fire speed and persistence in any given pixel, both a function of fuel loads and moisture content. We will quantify these relationships based on carefully selected Sentinel-2 image pairs and Sentinel-2 based burned area estimates from FireCCI, to establish small fire burned area for different agricultural systems and burned areas from fast moving fires along gradients of fuel availability. This will result in a set of scaling factors required to estimate burned area and subsequently fire emissions from open cover types. We will also provide similar estimates for forested systems, but there we expect much closer correspondence between burned area and fire perimeters (Oliva and Schroeder, 2015; Veraverbeke et al., 2014). We will use a random sample of Sentinel-2 pairs/FireCCI burned area across the study regions to evaluate accuracy, with the choice of products depending on availability. To avoid loss of sensitivity in rapidly recovering grasslands, images pairs will be about one month apart and will be used to evaluate burned area from selected fires that had both start and end dates within this period. One of the exciting outcomes of spatial maps of fire behaviour, type and size, is that these characteristics are likely closely related to both scaling factors and accuracy, translating in a direct understanding of regional product strengths and limitations. This step will enable direct estimates of fire emissions based on estimates of fuel loads and combustion completeness from a combination of modelling and top-down constraints.

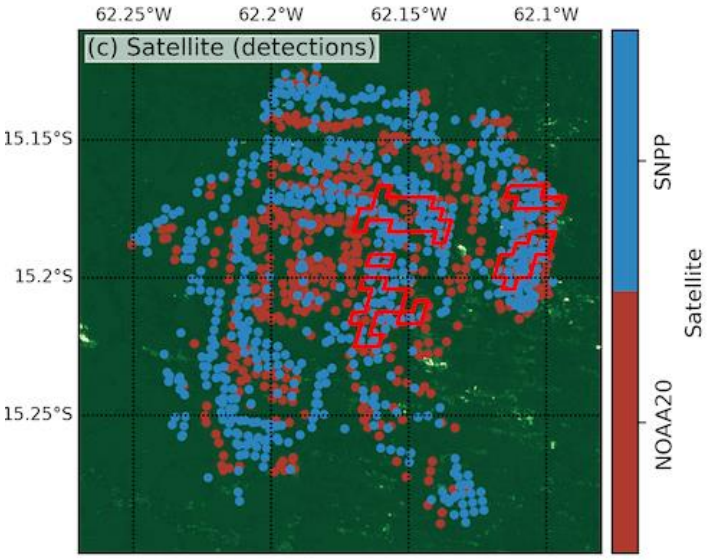

Figure 6: Alternating pattern of NOAA-20 and Suomi-NPP active fire detections for a forest fire event in the Amazon study region. This figure highlights the added value of combining active fire detections from multiple sensors and overpass times to detect burned area extent of low-intensity fires burning in tropical forest understorey. Red polygons highlight corresponding burned area estimates from the MCD64A1 burned area product.

3.2.3 Identification of fire behaviour and fire types

Compared to the existing algorithm that tracks daily fire perimeters, speed, and duration, the addition of Sentinel-3 data will strongly improve the characterisation of fire diurnal behaviour (FRP) and total fire radiated energy (FRE). We will combine data on fire behaviour and diurnal cycle with land cover characterisation and estimated fuel loads to improve the identification of regionally important fire types. The current approach was developed for southern America, and separates small clearing and agricultural fires, savannah fires, deforestation fires and forest fires. In addition to the fire characteristics, the algorithm includes information about tree cover (Hansen et al. 2013) and historic deforestation (PRODES) to identify specific fire types in the Amazon region. In southern hemisphere Africa, we will be particularly focused on separating fires associated with woodland and forest degradation from savannah or agricultural fires. Higher fuel loads result in distinct changes in the fire diurnal cycle, FRP, and fire persistence. In addition, we will use information about tree cover (Hansen et al. 2013) and landcover from the land cover cci to identify these regionally important fire types. In Russia it will be important to separate stand replacing crown fires, from forest understorey fires and other fire types associated with herbaceous fuels. It is generally assumed that crown-fires are less frequent in boreal Asia compared to North America, but regional patterns remain poorly understood. We will also use estimates of peatland and permafrost extent, to understand fire occurrence and behaviour of these specific fire types. Changes in surface reflectance following fires can greatly accelerate permafrost thawing. The fire type classification will be partly directly based on the different land cover mapping, but we will use pre- and

post-fire Sentinel-2 pairs and tree cover losses (Hansen et al., 2013) to further train and evaluate the algorithm. For example, we will use visual interpretation of tree mortality and fire severity indices to identify crown and understorey fires in the boreal region for algorithm training and validation purposes.

3.2.4 Quality assessment

For quality assessment of the burned area estimates, we will use the same approach as the original calibration, but based on a different random sample of Sentinel-2 tiles. For Africa, we will apply the same approach, but based on the existing Sentinel-2 burned area product for 2019. Quality assessment of the fire type classifications will initially remain a challenge, due to the lack of similar datasets or large-scale field data. However, for the Amazon region, we will compare our fire type estimates to those from the Monitoring of the Andean Amazon Project (MAAP). MAAP provides a smaller subset of different large fire events and their type based on visual interpretation of high-resolution satellite imagery. Our objective would be to start building a network of regional stakeholders and scientist with interest in the object-based fire tracking capability to aid further comparison to regional datasets that are not publicly available.

3.2.5 Risks and solutions

The quality assessment and validation components of the approach remain a challenge. We will mitigate this issue via various approaches. First, where possible, we will compare our findings to existing products like the FireCCI Sentinel-2 burned area product or MAAP. In addition, we will combine Sentinel-2 and active fire detections to visually interpret the extent of fires for calibration and validation. The subsequent uncertainty derived emissions estimates will be further constrained via top-down emissions estimates. In our experience developing the data for the Amazon region, the new datasets and subsequent use cases by scientist and regional stakeholders will also result in new validation and calibration opportunities as the project progresses.

3.3 Atmospheric composition

3.3.1 Emission datasets

In relation to emissions, we will use the following **datasets**:

- GFEDv4
- GFASv1.2 and GFASv1.4
- Injection height estimates from IS4FIRES and Plume Rise Model (PRM) modules.

The GFEDv4 (van der Werf et al., 2017) and GFASv1.2 (Kaiser et al., 2012) provide daily products of gridded fire emission estimates for a range of trace gases and aerosol.

GFASv1.4 is an updated version, which additionally provides an estimate for the diurnal cycle.

Two parameterisations for injection heights can be adopted in the global atmospheric chemistry module, namely the IS4Fires and PRM (Rémy et al., 2017), which provide the "mean altitude of maximum injection". By selecting different options for injection height, it is possible to assess the uncertainty of the model evaluation that originates from injection height assumptions.

The GFAS and GFED emission data serve as reference to be compared to the emissions product to be developed in this project. GFAS-based fire emissions are used operationally in the Copernicus Atmosphere Monitoring Service, routinely checked and updated following a development schedule. GFEDv4s can be considered as a main reference dataset that is widely used. A comprehensive analysis and inter-comparison of present-day emission products, including the ones discussed here, is reported in Pan et al. (2020). The range of spread in their reported emission estimates can be considered as an overall uncertainty. Nevertheless, the accuracy of individual emission products remains difficult to estimate, as it is region and time dependent, and furthermore can only indirectly be assessed through the use of a chemistry transport model.

3.3.2 Atmospheric composition observation data

Atmospheric composition observation data from Sentinel-5p will be used to provide top-down constraints on fire emissions. **Data products** used in this scope include:

- S-5p Trace gas observations of CO, tropospheric NO_2 and HCHO
- S-5p Aerosol observations of aerosol index, and aerosol layer height

S-5p observations of trace gases and aerosol are available daily at around 13:30h local time, with a horizontal resolution of approximately 5 km. The accuracy of tropospheric NO_2 and CO is considered sufficient for monitoring fire emission plumes down to the S-5p resolution of approximately 5 km on a daily basis (https://S-5p-mpc-vdaf.aeronomie.be/). Average S-5p HCHO measurements provide information on monthly time scales and longer

For tropospheric NO_2, the estimated accuracy meets the mission requirement of 50% for single pixel measurements. The current tropospheric NO_2 data product is biased low (estimated 22%) which is partly attributed to clouds. Efforts are in place to reduce the low bias. Note that daily tropospheric NO_2 columns cover more than two orders of magnitude depending in space and time. S-5p NO_2 data has already been shown to allow for detection of very small emissions plumes from single sources on a daily basis like gas-pipeline compressor stations (van der A et al., 2020) and under ideal conditions even individual ship plumes (Georgoulias et al., 2020).

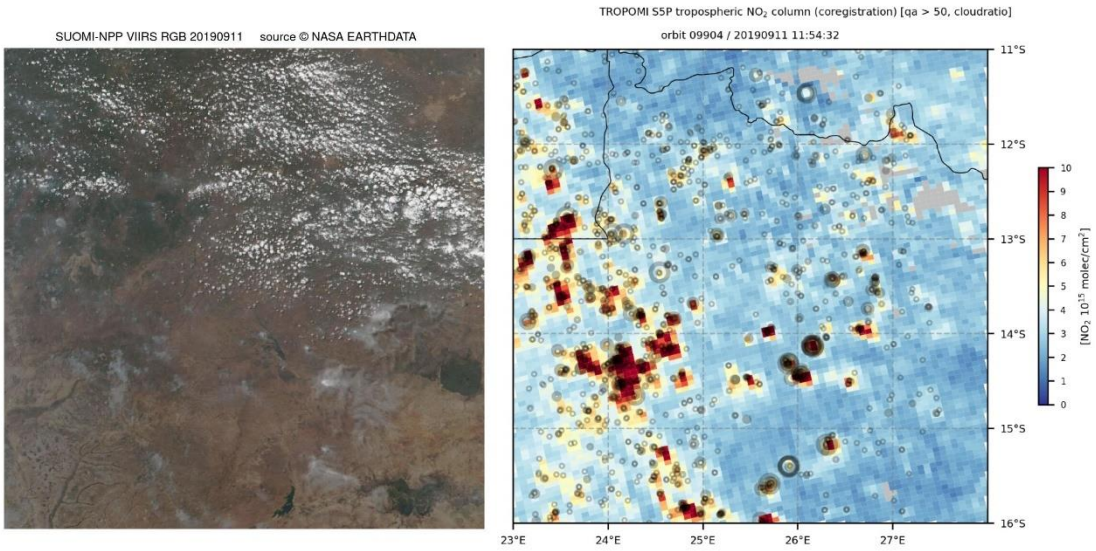

Figure 7: VIIRS pseudo-colour image (left) over the Sense4Fire Africa region and associated S-5p NO_2 measurements (right) for 11th September 2019. Indicated in the right plot are also the VIIRS fire radiative power measurements (green circles), with the circle diameter indicative of the fire radiative power amplitude. NO_2 measurements are resampled (coregistration) to the S-5p resolution of the Carbon Monoxide measurements.

For CO, the estimated accuracy meets the mission requirement of 15% bias and 10% accuracy for single measurements. The current CO data product bias is estimated at 6.5% with an accuracy of 5%. The current CO data product shows that there is a bias dependent on solar zenith angle, displays some orbital stripes, and underestimates CO for high pollution (5%). Note that daily CO columns cover an order of magnitude depending in space and time. First results reveal highly accurate CO measurements (Borsdorff et al., 2018b) down to a daily basis on city scales (Borsdorff et al., 2018a).

For HCHO, the estimated accuracy meets the mission requirement of 80% bias for single measurements. The current HCHO data product bias is estimated at approximately 30%, with a positive bias over clean areas and a negative bias over polluted areas. Note that due to the short atmospheric lifetime of HCHO and large spatial variability, the single measurement accuracy and precision are insufficient to use for single-pixel-scale monitoring. Rather, HCHO measurements need to be average in space and time to arrive at meaningful information. First results indicate that monthly mean S-5p HCHO provides sufficient spatial details for exploring its use and added value for Sense4Fire (see Vigouroux et al., 2020).

For S-5p data on aerosols, the AAI provides only qualitative product (location of absorbing aerosols and the relative strength of the absorption of shortwave radiation). AAI does however allow for identifying fire smoke plumes, which can be used to characterise an emission plume. Do note that due to the high spatial resolution of S-5p the AAI suffers from cloud edge and cloud shadow effects that precursor satellite missions OMI, GOME-

2, and SCIAMACHY, did not suffer from. These shadowing effects are related to the AAI being a non-physical parameter (two-wavelength ratio) and are difficult to resolve

For the S-5p ALH, the estimated accuracy meets the mission requirement of 1 km. Depending on the comparison dataset, the estimated bias ranges between 50-600 metres (Chimot et al., 2018; Nanda et al., 2020). A complicating factor for evaluating the S-5p ALH is the representative altitude of the measured height of an aerosol layer. S-5p measures the centroid ALH, whereas some comparison data provides heights close to the top of an aerosol layer. Evaluation of only very thick aerosol plumes indicates that the differences can decrease to 50 metres. Sense4Fire will consider these effects in evaluation aerosol layer heights, although it should be noted that evaluation of the ALH is ongoing so that Sense4Fire may have to develop a comparison strategy itself. The ALH accuracy can be rather low due to cloud contamination and surface effects. Improvement on these issues is part of ongoing research. In addition, the S-5p instrument time-dependent wavelength-dependent degradation affects AAI values, so the applied AAI filter for the ALH retrievals removes currently a large number of observations, which are in principle well suited for ALH retrievals. This may change in the future. Finally, comparison studies have revealed that the S-5p ALH currently has an upper altitude limit of approximately 13 km. The main reason for this is that such high aerosol clouds were not anticipated, so the retrieval algorithm was not designed for measuring ALH above 13 km. No improvements or updates on this particular issue are expected in the near future. However, it is not expected that such high altitude aerosol layers will be encountered for the areas and time periods that Sense4Fire will explore.

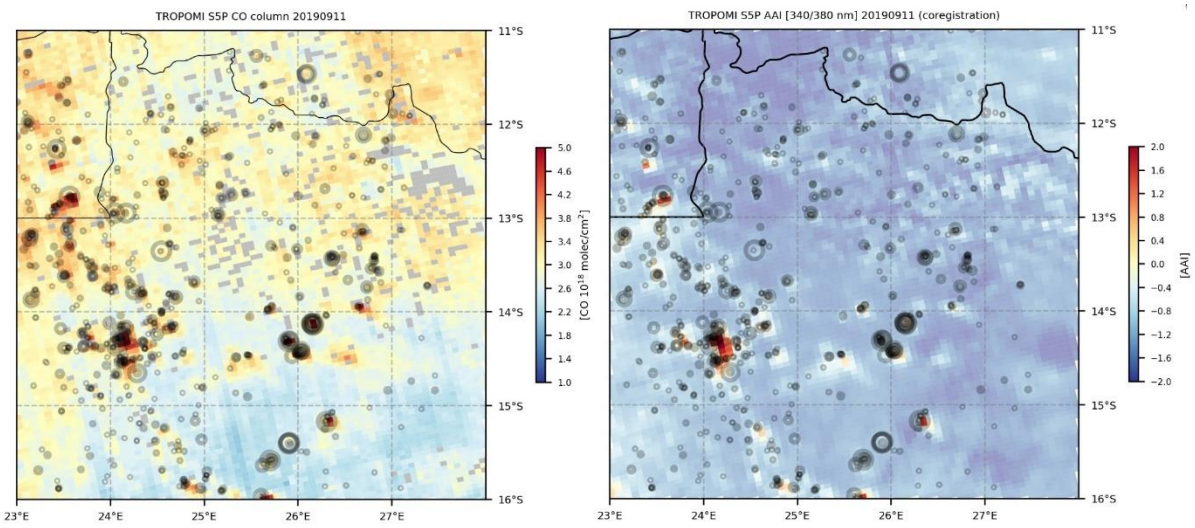

Figure 8: S-5p CO measurements (left) and S-5p AAI (right) for 11th September 2019. Indicated in the right plot are also the VIIRS fire radiative power measurements (green circles), with the circle diameter indicative of the fire

radiative power amplitude. AAI measurements are resampled (coregistration) to the S-5p resolution of the Carbon Monoxide measurements.

S-5p data will allow for individual fire based evaluation of NO_2 and CO plumes as well as their ratios, as along as the fire and associated emission plume is spatially sufficiently large so that it can be captured by S-5P. For longer-term averages, the cumulative effect of fires on average atmospheric composition can be further explored using HCHO. S-5p information on aerosols can further support data analysis and the comparison with model results.

The S-5p capacity to observed individual fire plumes will also allow for building a single-fire characteristic database consisting of S-5p data as well as well as fire information based on Sentinel-3 and Sentinel-2, like burned area, fire radiative power, fuel load, fuel type, and soil moisture. That would allow for detailed statistical analysis of fire characteristic of fire emissions based on these fire characteristics.

3.3.3 CAMS atmospheric composition model data

A model for atmospheric composition is necessary to be able to evaluate estimated emissions against satellite observations of atmospheric composition, i.e. to provide top-down constraints on fire emission estimates. For this we will exploit the atmospheric composition model developed within CAMS (Huijnen et al., 2019; Williams et al., 2021; Rémy et al., 2021). Specifically, this is intended to be the CY48R1-version of the IFS (CB05-AER) tropospheric chemistry and aerosol model configuration, which contains all the robust and comprehensive model updates that have been developed in the CAMS tenders on global chemistry and emissions over the course of 2019-2021. This model cycle is expected to be released for users by January 2022.

The **method** intended for the investigation of key sensitivities with respect to the top-down emission constraints, i.e. our scientific question on this project, starts with the definition of a reference model and evaluation configuration. Targeted sensitivity experiments will be setup to quantify sensitivities to model and emission parameterisations that contribute to uncertainties in the top-down constraints: tracer lifetime, injection height and emission factor through analysis of its estimated impact on atmospheric composition with respect to (S-5p) satellite observations. In addition, the model will provide top-down constraints on various iterations of biomass burning emission datasets as developed in this project (see Sec. 3.4).

The model output **datasets** consist of a range of diagnostics, including, in its standard configuration:

- 3-hourly, 3D datasets of trace gases, including CO, NO_2, CH_2O and O_3 on a 0.5-degree horizontal resolution

- 3-hourly, 3D datasets of aerosol concentration, including black carbon, organic carbon and secondary organic aerosol
- 3-hourly 2D fields of integrated AOD at various wavelengths, and additionally split out for individual aerosol components

These concentration datasets will be collocated in time and space with observational datasets, in particular the S-5p observations discussed above. This will allow quantitative assessment of model biases, which in turn can be associated to emission biases. For this purpose tropospheric and total columns will be computed from the model values, furthermore taking into account the averaging kernels which describe the satellite sensitivity to observed concentrations at different altitudes in the atmosphere. Finally, model data will be filtered for valid observations according to the quality flags. Cloudy pixels, with cloud radiance fraction> 0.5 will be omitted for NO_2 and HCHO observations. This procedure will allow for a fair inter-comparison between modelled and observed concentrations, although at the expense of observational data available for model evaluation.

3.3.4 Risks and solutions

We identify the following risks

- Uncertainties in reference emissions
- Gaps in satellite observations, e.g. due to clouds
- Limitations in accuracy of satellite retrievals (mainly HCHO)
- Model aspects.

These risks, together with their mitigation measures, are described in more detail below. Risks associated to **reference emissions**: sufficient baseline accuracy for sensitivity testing. One mitigation approach is that we are in contact with the developers of the GFAS system, which is the standard fire emission adopted in CAMS model simulations. If serious problems are identified this can be discussed with them to find a solution.

Risks associated to **satellite observations:**

1. missing data due to cloud and smoke. Solution: aggregation where needed*, updates of retrieval algorithms**
2. insufficient accuracy. Solution: aggregation where needed*
3. systematic biases: Solution: ad-hoc bias correction, updates of retrieval algorithms**

* based on current S-5p data product validation results aggregation for HCHO is mandatory even without missing data, see section 3.3.2.

**algorithm updates and switch in S-5p operational data processing is planned towards the end of 2021, reprocessing of past data with updated algorithms envisioned for summer 2022.

Risks with respect to **modelling aspects** consist of technical, and model accuracy-related risks:

1. A technical risk concerns the timely availability of a CY48R1 model configuration on ECMWF's supercomputing infrastructure. As found from experience, this is subject to technical delays that are outside the influence in this project. A general mitigation is to exploit a fall-back model configuration based on CY47R3.1, that is actually readily available which contains most of the desired new scientific updates, at least with regard to atmospheric composition aspects.
2. A second technical risk concerns the preparation of input emissions such that the model can ingest them. This is especially the case if input emission data files are not CF-compliant, and in earlier versions of the model which required input data in grib-format. The main mitigation measure includes the use of the latest 'flexible emissions' scripting software developed in CAMS, which allows ingestion of netcdf-based emission input data, to reduce the need for data-conversion. Furthermore, we will ensure that any data preparation will follow standard (CF-compliant) data conventions.
3. A scientific risk concerns whether the atmospheric composition model is fit-for-purpose, i.e. the model accuracy is sufficient. Persistent model biases – if not well characterised – obscure the analyses. General **mitigation** approaches consist of tuning and bias correction activities. For model tuning we benefit from activities taking place in CAMS during the preparation of the next operational model configuration, which is based on CY48R1. This also includes the selection of most appropriate reference anthropogenic, biogenic as well as biomass burning emissions. During the tuning stage a well-chosen set of model experiments will be executed, and evaluated against a range of standard observational datasets. This results in specification of an optimal model configuration for operational application in CAMS, but can equally be used to identify an optimal model configuration for this project.
   Considering that the model tuning activity described above focusses on global optimised configuration, local biases may persist. Therefor an additional **mitigation** activity concerns a characterisation of such model biases for the species, time periods and study regions of interest here, in particular with respect to the observations that are used for providing top-down constraints.

3.4 Estimating and validating fire emissions

3.4.1 Object-based fire emissions inventory

We will use the new dataset of individual fires to pilot the first "object-based" emissions inventory that characterises hourly emissions from individual fires during the different stages of their lifetime. Hourly resolution will be achieved based on a simple daily redistribution of emissions and the four daily active fire detections within the individual fire perimeters (following Kaiser et al., 2012). We will generate a five year record (2019 - 2023) of trace gas, aerosol and total carbon emissions for all identified individual fires in the four test areas (Brazil, southern Africa, and 2x Russia) and in one of the associated RECCAP-regions, following two steps. First, we will expand the dataset of individual fire perimeters, type, behaviour, and associated burned area across the three study regions (2019-2023) as described in section 3.2. Second, we will combine per-fire burned area estimates with estimates of fuel loads, moisture content and combustion completeness to derive carbon emissions estimates across the three study regions (2019-2023; section 3.1). Initially, we will use a standard set of emissions factors (e.g. Andreae, 2019) to derive emissions for a range of trace gases. However, estimates of carbon emissions and emissions factors are further constrained by top-down estimates of total carbon emissions, as explained in sections 3.3 and 3.4.2. Based on the optimisation against spatiotemporal patterns of the contribution of different fire types to overall emissions we will provide an optimised set of emissions factors for various representative fire types across the study regions. We will further explore the ability to scale emissions factors and injection heights dynamically based on fire behaviour. For example, by the end of September, almost 90% of active fire detection from the Amazon region originate from multi day fires, and over 60% from fires burning for over 10 days. Atmospheric conditions and wildfire behaviour change considerably during the night-time when smoke remains trapped near the surface. Improved characterisation of multi-day fires and their diurnal behaviour is therefore a critical step towards accurate modelling of smoke composition and transport. We will evaluate emissions estimates by comparison to existing emissions inventories and by integration within the CAMS framework for direct comparison to column measurements from TROPOMI (see section 3.4.3). Our object based approach and high temporal resolution also provide unique opportunities to compare results directly to emissions estimates from field campaigns or individual fire plumes, enabling novel ways of product validation.

3.4.2 Reconciling top-down and bottom-up emission estimates

The model simulation of atmospheric composition against the satellite observations at larger scale (both spatially and temporally) provides an important opportunity to feedback information from the top-down perspective towards the bottom-up approach.

For example, we will assess persistent biases in modelled trace gases in the atmosphere by disentangling the contribution from local emissions with background biases, particularly relevant for longer-lived trace gases such as CO. The resulting dataset will enable us to quantify potential biases of bottom-up carbon emissions estimates and emissions factors. In particular, we expect that observed biases between bottom-up and top-down emissions estimates will originate mostly from the combination of fuel consumption estimates and trace-gas specific emissions factors. Hence, we will follow van der Velde et al. (2021) to use the NO_2 / CO ratio as an indicator of combustion efficiency. Disentangling these components will enable us to simultaneously constrain total carbon emissions from the bottom up approach and optimise the standard emissions factors for our study regions. We will investigate the relationship between combustion efficiency and the spatiotemporal occurrence of different fire types across our study regions to derive a set of fire type specific emissions factors. We also expect to find relationships between fire behaviour and observations of combustion efficiency, and we will explore these where and when possible.

3.4.3 Quality assessment

The quality of estimated emissions from the proposed methods and approaches will be evaluated following three approaches.

First of all, the CAMS atmospheric model will be run covering the proposed regions and emission estimates as derived within Sense4Fire. For the selected regions, model results for NO_2, CO, and HCHO will be compared with Sentinel-5p observations from the same species, see example evaluation in Figure 9.

For these comparisons the model results will be sampled according to where on a daily basis Sentinel-5p measurements are available as clouds and data quality issues will lead to gaps in daily Sentinel-5p fields. Furthermore, averaging kernels will be applied to the corresponding model data.

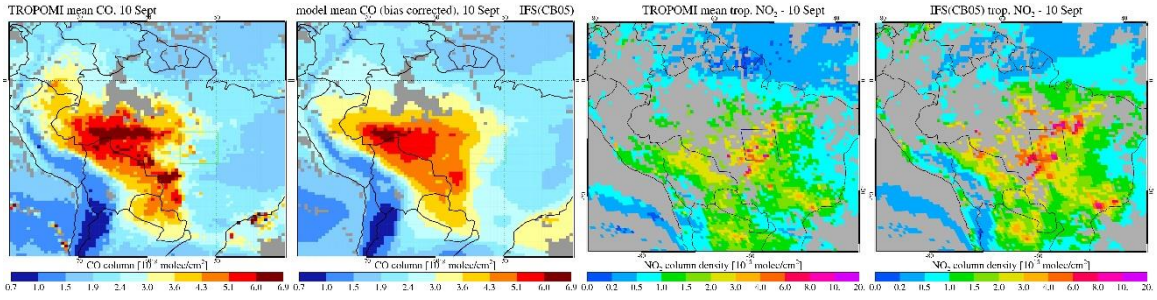

Figure 9: Example evaluation of CAMS model simulations against S-5p observations over the Amazon for 10th September 2020. Left two plots: S-5p and model CO; right two plots: S-5p and model NO_2.

Model results will then be averaged over time (monthly to seasonal) to compare with averaged observations. This model-observation comparison will in particular focus on

biases, spatial extent, and the ratio between various trace gases, as well as associated average vegetation type, fuels, soil moisture, bottom-up emissions (GFED, GFAS), to provide hints of causes for differences between observations and model results. Note that in particular the NO_2 and CO ratio may provide strong indications of emission characteristics as both products are associated with burning efficiency and fire temperatures (albeit inversely: more complete burning at higher temperatures will lead to more NO_2 and less CO, and vice versa for more incomplete burning at lower temperatures).

The modelled aerosol height will be compared with the Sentinel-5p observed aerosol layer height, but given the worse sampling of the ALH may be performed primarily on a case-to-case basis and/or statistically rather than using spatio-temporal averages.

For the observed absorbing aerosol index – which is a qualitative parameter and mostly used to identify aerosol plumes – results will be qualitatively compared with modelled aerosol plume extension on a daily basis and/or case-by-case basis, i.e. do spatial extents of modelled and observed smoke and aerosol plumes match.

In addition, first exploratory work may be done on constructing a large "single-fire" database consisting of individual fires and associated characteristics like vegetation type, fuels, soil moisture, and measurements of NO_2 and CO in the emission plumes. Statistical analyses of the fire characteristics of various fire types may reveal consistent characteristics for similar fires. Note that such exploratory work is not described in the Sense4Fire proposal but since it is very easy to construct such a database during the assessment process, it makes sense to explore whether there is added value in such an analysis, including single-fire characteristics data and information from Sentinel-1, Sentinel-2, and Sentinel-3.

3.4.4 Risks and solutions

Risks for the development of the fire-tracking algorithm are relatively low, as the concept was already demonstrated for the Amazon region. There is some risk associated with the new developments, for example, the quality of Sentinel-3 active fire products needs to be assessed and the extent to which the algorithm can be expanded to capture new fire types remains to be explored. The largest risk for Sentinel-3 might originate from the less precise estimates of fire location with 1 km nadir resolution, this could be mitigated by giving VIIRS data a higher priority for deriving fire perimeters, while Sentinel-3 active fires could still be used to provide context on the diurnal cycle and distribution of emissions estimates (or fire location if no VIIRS data is available). The risks related to fuel load and consumption estimates are described in more detail in section 3.1.5.

The reconciliation of the top down and bottom up approaches comes with some risk in the sense that this would further depend on the final quality of both bottom up and top-

down datasets. Moreover, there is a need to disentangle and investigate combustion efficiency for different fire types and environmental conditions. We expect that we can make a significant advance compared to existing approaches but also fully acknowledge that there will be limitations to our approach. One mitigation strategy would be to simplify the number of fire types into fire types that are easily separated in time and space for disentangling combustion efficiency and emissions factors. Similarly, we could consider investigating the seasonal variation in combustion efficiency and emissions factors rather than a per fire-type approach. In all instances, this would mostly affect the emissions estimates of various trace gases and less the estimates of total carbon emissions.

Risks and resolutions with regard to observations, emission databases, model simulations, and methods and approaches, are already discussed in sections 3.2.5 and 3.3.4.

4 Technical specification of the target products

The technical specifications of all target products are summarised in Table 1. The temporal coverage of the fuel load and moisture products will be from 2014 to 2021. The fire and emission products will be developed and tested for the years 2019 to 2023. All products will be developed, tested and applied for the four test areas. Finally, all products will be applied to one region of the Regional Carbon Cycle Assessment and Processes-2 (RECCAP-2) project, which will be either Brazil, southern hemisphere Africa or Siberia. The team will take this decision during the second phase of product development and validation by considering the performance and reliability of the different approaches in each test region.

Table 1: Overview about the technical specifications of the target products to be included in the Experimental Dataset

Name	Description	Minimum spatial and temporal resolution Temporal coverage	Optimum spatial and temporal resolution Temporal coverage
Fuel loads (FL) BM_tree_[leaves, wood] BM_herb	Biomass in different tree compartments and herbaceous vegetation Unit: kg/m²	Calibration of the approach at 0.25 x 0.25° Application to 1 x 1 km Monthly time step for canopy and herbaceous fuels, annual time steps for woody fuels	Calibration and application of the approach at 300 x 300 m 10-daily time step for canopy and herbaceous fuels, annual time steps for woody fuels

FL_[dead]_x	Mass of dead fuels, debris and organic material, Unit: kg/m²	Training of the machine learning model at 0.25 x 0.25° Application to 1 x 1 km Annual time step	Training and application of the machine learning model at 300 x 300 m Annual time step
Fuel moisture (FM) LFMC_[tree, herb] DFMC	Live-fuel moisture content of tree leaves and herbaceous vegetation, Unit: % Dead-fuel moisture content Unit: %	Estimation at 1 x 1 km Monthly time step Estimation at 10 x 10 km Monthly time step	Estimation at 300 x 300 m 10-daily time step Estimation at 1 x 1 km Daily time step
Fire objects Fire perimeters Active fires from S3 and VIIRS	Each fire perimeter will include attributes about fuel properties, fire behaviour, type, burned area and emissions estimates. Active fire detections with attributes, including unique fire identifying number, time, location, type of carbon emissions, and other relevant fire characteristics.	Fire object based Shapefile. Shapefile of active fire detections (minimum spatial accuracy 1 km, temporal: 10 am, 1:30 pm, 10 pm, 1:30 am).	Annual cumulative layer that can be updated in near-real time following availability of novel active fire detections. Annual cumulative layer that can be updated in near-real time following availability of novel active fire detections.
Fire emissions Trace gases	Emissions of key trace gases and aerosol. Unit: kg $m^{-2}s^{-1}$	Per-fire object (minimum object size about 30ha), temporal: 10 am, 1:30 pm, 10 pm, 1:30 am.	Annual cumulative layer that can be updated in near-real time following availability of novel active fire detections.

5 Scientific analyses

We will carry out three science cases that address the scientific questions as stated in chapter 1.2.

5.1 Assessing effects of fuel changes on fire behaviour

Previous studies have shown that antecedent FAPAR is one of the most important predictors for burned area (Kuhn-Régnier et al., 2021). This is likely because fuel build-up (i.e. higher FAPAR) can support larger fires. Here we aim to conduct a more detailed analysis of the role of fuels on fire behaviour. The objective of this science case is to obtain knowledge about how changes in tree, herbaceous and litter fuel loads and fuel moisture affect fire spread, fire size and fire severity at larger scales.

Therefore, we will use the fuel products from one or all study regions as predictors for fire spread, fire size and fire severity. Guided by our previous work (Forkel et al., 2019a), machine learning approaches such as random forest or deep learning methods such as long-/short-term memory networks (LSTMs) will be used to predict dynamics in fire behaviour from fuel properties and meteorological data. We will then apply methods from explainable machine learning such as partial dependencies or accumulated local effects,

permutation feature importance, and SHAP (SHapley Additive exPlanations) importance and dependencies, to visualise which and how fuel properties affect fire behaviour. The results will be compared with relations that are used in fire-enabled dynamic global vegetation models.

This analysis will provide novel insights in vegetation-fire interactions at large scales that can guide the development of global fire models. Such an analysis has not been possible because of the unavailability of datasets on fuel properties and fire behaviour.

5.2 Assessing effects of fires on short- and long-term carbon emissions

Fires have both direct and indirect effects on ecosystem carbon storage and biomass. Part of the biomass or "fuel" is consumed directly by the fire and emitted to the atmosphere as trace gasses and aerosols. In fire adapted ecosystems, like savannahs, direct combustion of fuels is the largest driver of carbon emissions, while ecosystems typically recover rapidly after fire. In frequently burning savannahs and grasslands biomass burning can be the dominant pathway of decomposition of organic material (Murphy et al., 2019). In ecosystems that are poorly adapted to fire, like humid-tropical forests, the direct emissions from fires burning the litter layer are limited, but fires can kill up to 50% of the above-ground biomass (Rappaport et al., 2018). In many ecosystems, including temperate and boreal forests, fires are occurring naturally but their frequency and intensity has changed over recent decades. Our hypothesis is that changing global fire regimes will have an increasing "indirect effect" on the global carbon cycle, due to committed carbon emissions that cannot be directly measured by the emissions of trace gases.

During this study we will track the carbon from direct emissions and due to committed emissions, particularly from tree mortality. The new individual fire database and associated fire types provide unique insights in the long-term implications of carbon emissions to the atmosphere. On the one hand, the dataset allows for separation of fires occurring in fire-adapted ecosystems with short carbon turnover times from fire, and non-fire adapted systems where fires cause long-term change. The fire types also provide direct information about the cause of fires, for example, carbon emissions from fires associated with deforestation or land-clearing will be the most permanent, with emissions from temperate or boreal forests slowly reabsorbed by the forests when they regrow. Even in fire-adapted systems, the ecosystem impacts will be governed by the fire temperature and severity, and the separation of crown and ground fires might prove a critical step towards understanding ecosystem impacts and recovery. Here we propose to characterise ecosystem impacts (e.g. tree mortality, total fuel consumption, changes in aboveground biomass) for a representative sample of each fire type. Subsequently, we will extrapolate our findings across the three study regions to understand the relative impacts of direct and indirect emissions across the different study areas.

Furthermore, we will also use the novel fire behaviour data to constrain simulations of the LPJmL-SPITFIRE fire model. Specifically, the statistical distributions of our estimates of fire behaviour (e.g. fire speed), combustion and emissions can constrain model processes such as rate of spread, and the combustion and emission calculations. In a previous analysis, we integrated several satellite datasets of FAPAR, sun-induced fluorescence, above-ground biomass, land cover and burned area with LPJmL to constrain model parameters for phenology, photosynthesis, biomass allocation and disturbance (Forkel et al., 2019a). This helped us to constrain model simulations of plant productivity, biomass and land carbon turnover. By redoing this analysis with the novel fire behaviour products, we will be able to quantify from the model the impacts of short- and long-term fire emissions on the overall land carbon sink capacity.

5.3 Assessment of the fire emission estimates and comparison with other approaches

The gridded emissions estimates will be compared with existing fire emission systems (GFED, GFAS) with the objective of disentangling and understanding the reasons behind observed differences. This aims to provide critical information which enable the improvement of existing systems and highlights strengths and limitations of our novel products developed here. We expect particularly large differences based on the more accurate separation of different fire types and associated changes in combustion completeness and emissions factors derived here.

An analysis of the use of atmospheric composition model simulations, varying different aspects (injection height, chemistry model details, and emission factor per fire type) will be performed and compared against S-5p satellite retrievals to assess its impact on the analysis. This relies furthermore on an analysis of trace gas and aerosol enhancements in S-5p observations that may be attributed to fires, which will be pursued first. In combination this provides a handle on various uncertainties that drive top-down methods to constrain fire emissions.

Finally, an impact analysis will be done by setting up a twin model simulation with GFAS reference, and Sense4Fire optimised fire emissions. Evaluation will be performed using the same set of observations as adopted for assessment of optimised emission estimates. This impact analysis will identify to what extent our optimised fire emissions leads to differences in model performance with respect to the observations.

6 Related European and international projects and activities

The main European and international projects and initiatives that are relevant for Sense4Fire and the area of potential collaboration are listed in Table 2.

Table 2: Related projects and activities

Project or initiative	Contact	Potential collaboration
ESA Carbon Science Cluster	The group has several contacts to members of other projects of the ESA Carbon Science Cluster	The BIOMASCAT product will be explored as input dataset to estimate fuel loads. Estimates of GPP from SEN4GPP will be considered as input for fuel accumulation.
H2020 FirEUrisk Developing a Holistic, Risk-wise Strategy for European Wildfire Management	TUD (M. Forkel and C. Marrs) are leading WP4 (Multi-level integration) and contribute to WPs 1 (fire risk assessment), 3 (mitigation to future fires) and 5 (test sites)	New products on fuel properties will be developed for Europe, these datasets can be used as further benchmark for the fuel products in Sense4Fire (e.g. novel fuelbed maps, retrievals of LFMC from S-3)
Leverhulme Centre for Wildfires, Environment and Society	M. Forkel is an associated international partner to the Leverhulme Centre	Products from Sense4Fire can be adopted within scientific studies at the centre.
ORNL Community Fire Database Network	The Oak Ridge National Laboratory is developing a community with the aim to build a global database on fire: https://apfire.wixsite.com/database M. Forkel was invited to this community.	
FWF/DFG FURNACES Fire in the Future: Interactions with Ecosystems and Society	TUD collaborates in this project with TU Wien, BOKU Vienna, Senckenberg and KIT to better model human effects on fires in DGVMs	The novel products in Sense4Fire can adapted as new benchmark datasets in DGVMs
DFG RECOVERY Recent changes in Northern Vegetation Carbon Cycling	TUD collaborates in this project with Uni Augsburg and PIK Potsdam	Use of novel satellite datasets of vegetation change in Siberia and of DGVM model simulations
CAMS Copernicus Atmosphere Monitoring Service	KNMI is involved in the further development of global atmospheric composition modelling.	Shared analysis of model-observation biases.
Fire Modelling Inter-comparison Project	N. Andela and M. Forkel are long-term collaborators in the FireMIP project.	Our new data can be used for benchmarking fire models as part of DGVMs.

7 Publication plan

The evolving plan of the proposed publications that are to be generated during the project and their estimated submission dates are shown in Table 3.

Table 3: Proposed publication plan

#	Working title	Objective / link to proposal	Lead	Estimated submission time
1	Estimating temporal dynamics of fuel loads by integrating various Earth observation datasets	Describe developments and validation of fuel load and moisture products	TUD (C. Wessollek, M. Forkel)	Oct 2022
2	Effects of land cover changes on fuel properties and fire behaviour	Describe analysis and results related to science question 1	TUD (M. Forkel, C. Wessollek)	Jul 2023
3	An object oriented approach to track wildfires in near-real time	Develop novel fire products.	CU (N. Andela and A. Awotwi)	Oct 2022
4	Consequences of fire for the global carbon cycle	Quantify 'emissions lifetime' to understand the cumulative evolving impact of fire on the Earth System (high-impact).	CU (N. Andela and A. Awotwi)	Jul 2023
5	What can we learn from S-5p observations of fire smoke plumes?	S-5p based characterisation of trace gas/aerosol enhancements due to fires)	KNMI (J. De Laat)	Oct 2022
6	Uncertainties in top-down fire emission constraints: reconciling model simulations with satellite observations	Describe key uncertainties that influence the top-down emission estimates	KNMI (V. Huijnen, J. de Laat)	May 2023

References

van der A, R. J., de Laat, A. T. J., Ding, J., and Eskes, H. J.: Connecting the dots: NOx emissions along a West Siberian natural gas pipeline, Npj Clim. Atmospheric Sci., 3, 1–7, https://doi.org/10.1038/s41612-020-0119-z, 2020.

Abbott, K. N., Leblon, B., Staples, G. C., Maclean, D. A., and Alexander, M. E.: Fire danger monitoring using RADARSAT-1 over northern boreal forests, Int. J. Remote Sens., 28, 1317–1338, https://doi.org/10.1080/01431160600904956, 2007.

Andela, N., Morton, D. C., Giglio, L., Chen, Y., Werf, G. R. van der, Kasibhatla, P. S., DeFries, R. S., Collatz, G. J., Hantson, S., Kloster, S., Bachelet, D., Forrest, M., Lasslop, G., Li, F., Mangeon, S., Melton, J. R., Yue, C., and Randerson, J. T.: A human-driven decline in global burned area, Science, 356, 1356–1362, https://doi.org/10.1126/science.aal4108, 2017.

Andela, N., Morton, D. C., Giglio, L., Paugam, R., Chen, Y., Hantson, S., Van Der Werf, G. R., and Randerson, J. T.: The Global Fire Atlas of individual fire size, duration, speed and direction, Earth Syst. Sci. Data, 11, 529–552, 2019.

Andreae, M. O.: Emission of trace gases and aerosols from biomass burning–an updated assessment, Atmospheric Chem. Phys., 19, 8523–8546, 2019.

Andreae, M. O. and Merlet, P.: Emission of trace gases and aerosols from biomass burning, Glob. Biogeochem. Cycles, 15, 955–966, https://doi.org/10.1029/2000GB001382, 2001.

Aragão, L. E. O. C., Anderson, L. O., Fonseca, M. G., Rosan, T. M., Vedovato, L. B., Wagner, F. H., Silva, C. V. J., Junior, C. H. L. S., Arai, E., Aguiar, A. P., Barlow, J., Berenguer, E., Deeter, M. N., Domingues, L. G., Gatti, L., Gloor, M., Malhi, Y., Marengo, J. A., Miller, J. B., Phillips, O. L., and Saatchi, S.: 21st Century drought-related fires counteract the decline of Amazon deforestation carbon emissions, Nat. Commun., 9, 1–12, https://doi.org/10.1038/s41467-017-02771-y, 2018.

Arora, V. K. and Melton, J. R.: Reduction in global area burned and wildfire emissions since 1930s enhances carbon uptake by land, Nat. Commun., 9, 1326, https://doi.org/10.1038/s41467-018-03838-0, 2018.

Avitabile, V., Herold, M., Heuvelink, G. B. M., Lewis, S. L., Phillips, O. L., Asner, G. P., Armston, J., Ashton, P. S., Banin, L., Bayol, N., Berry, N. J., Boeckx, P., Jong, B. H. J., DeVries, B., Girardin, C. A. J., Kearsley, E., Lindsell, J. A., Lopez-Gonzalez, G., Lucas, R., Malhi, Y., Morel, A., Mitchard, E. T. A., Nagy, L., Qie, L., Quinones, M. J., Ryan, C. M., Ferry, S. J. W., Sunderland, T., Laurin, G. V., Gatti, R. C., Valentini, R., Verbeeck, H., Wijaya, A., and Willcock, S.: An integrated pan-tropical biomass map using multiple reference datasets, Glob. Change Biol., https://doi.org/10.1111/gcb.13139, 2016.

Baccini, A., Goetz, S. J., Walker, W. S., Laporte, N. T., Sun, M., Sulla-Menashe, D., Hackler, J., Beck, P. S. A., Dubayah, R., Friedl, M. A., Samanta, S., and Houghton, R. A.: Estimated carbon dioxide emissions from tropical deforestation improved by carbon-density maps, Nat. Clim. Change, 2, 182–185, https://doi.org/10.1038/nclimate1354, 2012.

Barlow, J., Berenguer, E., Carmenta, R., and França, F.: Clarifying Amazonia's burning crisis, Glob. Change Biol., 26, 319–321, https://doi.org/10.1111/gcb.14872, 2020.

Barrett, K., Baxter, R., Kukavskaya, E., Balzter, H., Shvetsov, E., and Buryak, L.: Postfire recruitment failure in Scots pine forests of southern Siberia, Remote Sens. Environ., 237, 111539, https://doi.org/10.1016/j.rse.2019.111539, 2020.

Bauer-Marschallinger, B., Freeman, V., Cao, S., Paulik, C., Schaufler, S., Stachl, T., Modanesi, S., Massari, C., Ciabatta, L., Brocca, L., and Wagner, W.: Toward Global Soil Moisture Monitoring With Sentinel-1: Harnessing Assets and Overcoming Obstacles, IEEE Trans. Geosci. Remote Sens., 57, 520–539, https://doi.org/10.1109/TGRS.2018.2858004, 2019.

Bauwens, M., Stavrakou, T., Müller, J.-F., De Smedt, I., Van Roozendael, M., Van Der Werf, G. R., Wiedinmyer, C., Kaiser, J. W., Sindelarova, K., and Guenther, A.: Nine years of global hydrocarbon emissions based on source inversion of OMI formaldehyde observations, 2016.

Beck, P. S. A., Atzberger, C., Høgda, K. A., Johansen, B., and Skidmore, A. K.: Improved monitoring of vegetation dynamics at very high latitudes: A new method using MODIS NDVI, Remote Sens. Environ., 100, 321–334, https://doi.org/10.1016/j.rse.2005.10.021, 2006.

Boer, M. M., de Dios, V. R., and Bradstock, R. A.: Unprecedented burn area of Australian mega forest fires, Nat. Clim. Change, 10, 171–172, 2020.

Borsdorff, T., aan de Brugh, J., Hu, H., Hasekamp, O., Sussmann, R., Rettinger, M., Hase, F., Gross, J., Schneider, M., Garcia, O., Stremme, W., Grutter, M., Feist, D. G., Arnold, S. G., De Mazière, M., Kumar Sha, M., Pollard, D. F., Kiel, M., Roehl, C., Wennberg, P. O., Toon, G. C., and Landgraf, J.: Mapping carbon monoxide pollution from space down to city scales with daily global coverage, Atmospheric Meas. Tech., 11, 5507–5518, https://doi.org/10.5194/amt-11-5507-2018, 2018a.

Borsdorff, T., Aan de Brugh, J., Hu, H., Aben, I., Hasekamp, O., and Landgraf, J.: Measuring Carbon Monoxide With TROPOMI: First Results and a Comparison With ECMWF-IFS Analysis Data, Geophys. Res. Lett., 45, 2826–2832, https://doi.org/10.1002/2018GL077045, 2018b.

Brando, P., Soares-Filho, B., Rodrigues, L., Assunção, A., Morton, D., Tuchschneider, D., Fernandes, E., Macedo, M., Oliveira, U., and Coe, M.: The gathering firestorm in southern Amazonia, Sci. Adv., 6, eaay1632, 2020.

Chimot, J., Veefkind, J. P., Vlemmix, T., and Levelt, P. F.: Spatial distribution analysis of the OMI aerosol layer height: a pixel-by-pixel comparison to CALIOP observations, Atmospheric Meas. Tech., 11, 2257–2277, https://doi.org/10.5194/amt-11-2257-2018, 2018.

Chuvieco, E., Riaño, D., Aguado, I., and Cocero, D.: Estimation of fuel moisture content from multitemporal analysis of Landsat Thematic Mapper reflectance data: Applications in fire danger assessment, Int. J. Remote Sens., 23, 2145–2162, https://doi.org/10.1080/01431160110069818, 2002.

Di Giuseppe, F., Benedetti, A., Coughlan, R., Vitolo, C., and Vuckovic, M.: A Global Bottom-Up Approach to Estimate Fuel Consumed by Fires Using Above Ground Biomass Observations, Geophys. Res. Lett., 48, e2021GL095452, https://doi.org/10.1029/2021GL095452, 2021.

Falster, D. S., Duursma, R. A., Ishihara, M. I., Barneche, D. R., FitzJohn, R. G., Vårhammar, A., Aiba, M., Ando, M., Anten, N., Aspinwall, M. J., Baltzer, J. L., Baraloto, C., Battaglia, M., Battles, J. J., Bond-Lamberty, B., van Breugel, M., Camac, J., Claveau, Y., Coll, L., Dannoura, M., Delagrange, S., Domec, J.-C., Fatemi, F., Feng, W., Gargaglione, V., Goto, Y., Hagihara, A., Hall, J. S., Hamilton, S., Harja, D., Hiura, T., Holdaway, R., Hutley, L. S., Ichie, T., Jokela, E. J., Kantola, A., Kelly, J. W. G., Kenzo, T., King, D., Kloeppel, B. D., Kohyama, T., Komiyama, A., Laclau, J.-P., Lusk, C. H., Maguire, D. A., le Maire, G., Mäkelä, A., Markesteijn, L., Marshall, J., McCulloh, K., Miyata, I., Mokany, K., Mori, S., Myster, R. W., Nagano, M., Naidu, S. L., Nouvellon, Y., O'Grady, A. P., O'Hara, K. L., Ohtsuka, T., Osada, N., Osunkoya, O. O., Peri, P. L., Petritan, A. M., Poorter, L., Portsmuth, A., Potvin, C., Ransijn, J., Reid, D., Ribeiro, S. C., Roberts, S. D., Rodríguez, R., Saldaña-Acosta, A., Santa-Regina, I., Sasa, K., Selaya, N. G., Sillett, S. C., Sterck, F., Takagi, K., Tange, T., Tanouchi, H., Tissue, D., Umehara, T., Utsugi, H., Vadeboncoeur, M. A., Valladares, F., Vanninen, P., Wang, J.

R., Wenk, E., Williams, R., de Aquino Ximenes, F., Yamaba, A., Yamada, T., Yamakura, T., Yanai, R. D., and York, R. A.: BAAD: a Biomass And Allometry Database for woody plants, Ecology, 96, 1445–1445, https://doi.org/10.1890/14-1889.1, 2015.

Fan, L., Wigneron, J.-P., Xiao, Q., Al-Yaari, A., Wen, J., Martin-StPaul, N., Dupuy, J.-L., Pimont, F., Al Bitar, A., Fernandez-Moran, R., and Kerr, Y. H.: Evaluation of microwave remote sensing for monitoring live fuel moisture content in the Mediterranean region, Remote Sens. Environ., 205, 210–223, https://doi.org/10.1016/j.rse.2017.11.020, 2018.

Forkel, M., Migliavacca, M., Thonicke, K., Reichstein, M., Schaphoff, S., Weber, U., and Carvalhais, N.: Codominant water control on global interannual variability and trends in land surface phenology and greenness, Glob. Change Biol., 21, 3414–3435, https://doi.org/10.1111/gcb.12950, 2015.

Forkel, M., Dorigo, W., Lasslop, G., Teubner, I., Chuvieco, E., and Thonicke, K.: A data-driven approach to identify controls on global fire activity from satellite and climate observations (SOFIA V1), Geosci. Model Dev., 10, 4443–4476, https://doi.org/10.5194/gmd-10-4443-2017, 2017.

Forkel, M., Andela, N., Harrison, S. P., Lasslop, G., Marle, M. van, Chuvieco, E., Dorigo, W., Forrest, M., Hantson, S., Heil, A., Li, F., Melton, J., Sitch, S., Yue, C., and Arneth, A.: Emergent relationships with respect to burned area in global satellite observations and fire-enabled vegetation models, Biogeosciences, 16, 57–76, https://doi.org/10.5194/bg-16-57-2019, 2019a.

Forkel, M., Dorigo, W. A., Lasslop, G., Chuvieco, E., Hantson, S., Heil, A., Teubner, I., Thonicke, K., and Harrison, S. P.: Recent global and regional trends in burned area and their compensating environmental controls, Environ. Res. Commun., https://doi.org/10.1088/2515-7620/ab25d2, 2019b.

Frappart, F., Wigneron, J.-P., Li, X., Liu, X., Al-Yaari, A., Fan, L., Wang, M., Moisy, C., Le Masson, E., Aoulad Lafkih, Z., Vallé, C., Ygorra, B., and Baghdadi, N.: Global Monitoring of the Vegetation Dynamics from the Vegetation Optical Depth (VOD): A Review, Remote Sens., 12, 2915, https://doi.org/10.3390/rs12182915, 2020.

Freeborn, P. H., Wooster, M. J., Hao, W. M., Ryan, C. A., Nordgren, B. L., Baker, S. P., and Ichoku, C.: Relationships between energy release, fuel mass loss, and trace gas and aerosol emissions during laboratory biomass fires, J. Geophys. Res. Atmospheres, 113, https://doi.org/10.1029/2007JD008679, 2008.

Fuster, B., Sánchez-Zapero, J., Camacho, F., García-Santos, V., Verger, A., Lacaze, R., Weiss, M., Baret, F., and Smets, B.: Quality Assessment of PROBA-V LAI, fAPAR and fCOVER Collection 300 m Products of Copernicus Global Land Service, Remote Sens., 12, 1017, https://doi.org/10.3390/rs12061017, 2020a.

Fuster, B., Sánchez-Zapero, J., Camacho, F., García-Santos, V., Verger, A., Lacaze, R., Weiss, M., Baret, F., and Smets, B.: Quality Assessment of PROBA-V LAI, fAPAR and fCOVER Collection 300 m Products of Copernicus Global Land Service, Remote Sens., 12, 1017, https://doi.org/10.3390/rs12061017, 2020b.

Georgoulias, A. K., Boersma, K. F., Vliet, J. van, Zhang, X., A, R. van der, Zanis, P., and Laat, J. de: Detection of NO2 pollution plumes from individual ships with the TROPOMI/S-5P satellite sensor, Environ. Res. Lett., 15, 124037, https://doi.org/10.1088/1748-9326/abc445, 2020.

Giglio, L., Boschetti, L., Roy, D. P., Humber, M. L., and Justice, C. O.: The Collection 6 MODIS burned area mapping algorithm and product, Remote Sens. Environ., 217, 72–85, 2018.

Hansen, M. C., Potapov, P. V., Moore, R., Hancher, M., Turubanova, S. A., Tyukavina, A., Thau, D., Stehman, S., Goetz, S. J., Loveland, T. R., and others: High-resolution global maps of 21st-century forest cover change, science, 342, 850–853, 2013.

Hantson, S., Arneth, A., Harrison, S. P., Kelley, D. I., Prentice, I. C., Rabin, S. S., Archibald, S., Mouillot, F., Arnold, S. R., Artaxo, P., Bachelet, D., Ciais, P., Forrest, M., Friedlingstein, P., Hickler, T., Kaplan, J. O., Kloster, S., Knorr, W., Lasslop, G., Li, F., Mangeon, S., Melton, J. R., Meyn, A., Sitch, S., Spessa, A., van der Werf, G. R., Voulgarakis, A., and Yue, C.: The status and challenge of global fire modelling, Biogeosciences, 13, 3359–3375, https://doi.org/10.5194/bg-13-3359-2016, 2016.

Hantson, S., Kelley, D. I., Arneth, A., Harrison, S. P., Archibald, S., Bachelet, D., Forrest, M., Hickler, T., Lasslop, G., Li, F., Mangeon, S., Melton, J. R., Nieradzik, L., Rabin, S. S., Prentice, I. C., Sheehan, T., Sitch, S., Teckentrup, L., Voulgarakis, A., and Yue, C.: Quantitative assessment of fire and vegetation properties in simulations with fire-enabled vegetation models from the Fire Model Intercomparison Project, Geosci. Model Dev., 13, 3299–3318, https://doi.org/10.5194/gmd-13-3299-2020, 2020.

Holland, E. A., Post, W. M., Matthews, E. G., Sulzman, J. M., Staufer, R., and Krankina, O. N.: A Global Database of Litterfall Mass and Litter Pool Carbon and Nutrients, https://doi.org/10.3334/ORNLDAAC/1244, 2014.

Hooghiemstra, P., Krol, M., Meirink, J., Bergamaschi, P., Van Der Werf, G., Novelli, P., Aben, I., and Röckmann, T.: Optimizing global CO emission estimates using a four-dimensional variational data assimilation system and surface network observations, Atmospheric Chem. Phys., 11, 4705–4723, 2011.

Huijnen, V., Wooster, M. J., Kaiser, J. W., Gaveau, D. L., Flemming, J., Parrington, M., Inness, A., Murdiyarso, D., Main, B., and Van Weele, M.: Fire carbon emissions over maritime southeast Asia in 2015 largest since 1997, Sci. Rep., 6, 26886, 2016.

Huijnen, V., Pozzer, A., Arteta, J., Brasseur, G. P., Bouarar, I., Chabrillat, S., Christophe, Y., Doumbia, T., Flemming, J., Guth, J., and others: Quantifying uncertainties due to chemistry modelling: Evaluation of tropospheric composition simulations in the CAMS model (cycle 43R1), Geosci. Model Dev., 12, 1725–1752, 2019.

Ichoku, C. and Ellison, L.: Global top-down smoke-aerosol emissions estimation using satellite fire radiative power measurements, Atmospheric Chem. Phys., 14, 6643–6667, https://doi.org/10.5194/acp-14-6643-2014, 2014.

Kaiser, J. W., Heil, A., Andreae, M. O., Benedetti, A., Chubarova, N., Jones, L., Morcrette, J.-J., Razinger, M., Schultz, M. G., Suttie, M., and van der Werf, G. R.: Biomass burning emissions estimated with a global fire assimilation system based on observed fire radiative power, Biogeosciences, 9, 527–554, https://doi.org/10.5194/bg-9-527-2012, 2012.

Kaufman, Y. J., Tanré, D., and Boucher, O.: A satellite view of aerosols in the climate system, Nature, 419, 215–223, https://doi.org/10.1038/nature01091, 2002.

Knorr, W., Kaminski, T., Arneth, A., and Weber, U.: Impact of human population density on fire frequency at the global scale, Biogeosciences, 11, 1085–1102, https://doi.org/10.5194/bg-11-1085-2014, 2014.

Konings, A. G., Holtzman, N. M., Rao, K., Xu, L., and Saatchi, S. S.: Interannual Variations of Vegetation Optical Depth are Due to Both Water Stress and Biomass Changes, Geophys. Res. Lett., 48, e2021GL095267, https://doi.org/10.1029/2021GL095267, 2021.

Konovalov, I., Berezin, E., Ciais, P., Broquet, G., Beekmann, M., Hadji-Lazaro, J., Clerbaux, C., Andreae, M., Kaiser, J., and Schulze, E. D.: Constraining CO_2 emissions from open biomass burning by satellite observations of co-emitted species: a method and its application to wildfires in Siberia, Atmospheric Chem. Phys., 14, 10383–10410, 2014.

Kuhn-Régnier, A., Voulgarakis, A., Nowack, P., Forkel, M., Prentice, I. C., and Harrison, S. P.: The importance of antecedent vegetation and drought conditions as global drivers of burnt area, Biogeosciences, 18, 3861–3879, https://doi.org/10.5194/bg-18-3861-2021, 2021.

Lamarche, C., Santoro, M., Bontemps, S., D'Andrimont, R., Radoux, J., Giustarini, L., Brockmann, C., Wevers, J., Defourny, P., and Arino, O.: Compilation and Validation of SAR and Optical Data Products for a Complete and Global Map of Inland/Ocean Water Tailored to the Climate Modeling Community, Remote Sens., 9, 36, https://doi.org/10.3390/rs9010036, 2017.

Landgraf, J., aan de Brugh, J., Scheepmaker, R., Borsdorff, T., Hu, H., Houweling, S., Butz, A., Aben, I., and Hasekamp, O.: Carbon monoxide total column retrievals from TROPOMI shortwave infrared measurements, Atmospheric Meas. Tech., 9, 4955–4975, https://doi.org/10.5194/amt-9-4955-2016, 2016.

Lasslop, G., Coppola, A. I., Voulgarakis, A., Yue, C., and Veraverbeke, S.: Influence of Fire on the Carbon Cycle and Climate, Curr. Clim. Change Rep., https://doi.org/10.1007/s40641-019-00128-9, 2019.

Lasslop, G., Hantson, S., Harrison, S. P., Bachelet, D., Burton, C., Forkel, M., Forrest, M., Li, F., Melton, J. R., Yue, C., Archibald, S., Scheiter, S., Arneth, A., Hickler, T., and Sitch, S.: Global ecosystems and fire: Multi-model assessment of fire-induced tree-cover and carbon storage reduction, Glob. Change Biol., https://doi.org/10.1111/gcb.15160, 2020.

Leblon, B., Kasischke, E., Alexander, M., Doyle, M., and Abbott, M.: Fire Danger Monitoring Using ERS-1 SAR Images in the Case of Northern Boreal Forests, Nat. Hazards, 27, 231–255, https://doi.org/10.1023/A:1020375721520, 2002.

van Leeuwen, T. T., van der Werf, G. R., Hoffmann, A. A., Detmers, R. G., Rücker, G., French, N. H. F., Archibald, S., Carvalho Jr., J. A., Cook, G. D., de Groot, W. J., Hély, C., Kasischke, E. S., Kloster, S., McCarty, J. L., Pettinari, M. L., Savadogo, P., Alvarado, E. C., Boschetti, L., Manuri, S., Meyer, C. P., Siegert, F., Trollope, L. A., and Trollope, W. S. W.: Biomass burning fuel consumption rates: a field measurement database, Biogeosciences, 11, 7305–7329, https://doi.org/10.5194/bg-11-7305-2014, 2014.

Lizundia-Loiola, J., Franquesa, M., Boettcher, M., Kirches, G., Pettinari, M. L., and Chuvieco, E.: Implementation of the Burned Area Component of the Copernicus Climate Change Service: From MODIS to OLCI Data, Remote Sens., 13, 4295, https://doi.org/10.3390/rs13214295, 2021.

Mialon, A., Rodríguez-Fernández, N. J., Santoro, M., Saatchi, S., Mermoz, S., Bousquet, E., and Kerr, Y. H.: Evaluation of the Sensitivity of SMOS L-VOD to Forest Above-Ground Biomass at Global Scale, Remote Sens., 12, 1450, https://doi.org/10.3390/rs12091450, 2020.

Moesinger, L., Dorigo, W., Jeu, R. de, Schalie, R. van der, Scanlon, T., Teubner, I., and Forkel, M.: The global long-term microwave Vegetation Optical Depth Climate Archive (VODCA), Earth Syst. Sci. Data, 12, 177–196, https://doi.org/10.5194/essd-12-177-2020, 2020.

Murphy, B. P., Prior, L. D., Cochrane, M. A., Williamson, G. J., and Bowman, D. M.: Biomass consumption by surface fires across Earth's most fire prone continent, Glob. Change Biol., 25, 254–268, 2019.

Nanda, S., Graaf, M. de, Veefkind, J. P., Sneep, M., Linden, M. ter, Sun, J., and Levelt, P. F.: A first comparison of TROPOMI aerosol layer height (ALH) to CALIOP data, Atmospheric Meas. Tech., 13, 3043–3059, 2020.

Oliva, P. and Schroeder, W.: Assessment of VIIRS 375 m active fire detection product for direct burned area mapping, Remote Sens. Environ., 160, 144–155, 2015.

Ottmar, R. D., Sandberg, D. V., Riccardi, C. L., and Prichard, S. J.: An overview of the Fuel Characteristic Classification System — Quantifying, classifying, and creating fuelbeds for resource planning, Can. J. For. Res., 37, 2383–2393, https://doi.org/10.1139/X07-077, 2007.

Pan, X., Ichoku, C., Chin, M., Bian, H., Darmenov, A., Colarco, P., Ellison, L., Kucsera, T., da Silva, A., Wang, J., Oda, T., and Cui, G.: Six global biomass burning emission datasets: intercomparison and application in one global aerosol model, Atmospheric Chem. Phys., 20, 969–994, https://doi.org/10.5194/acp-20-969-2020, 2020.

Park, K., Emmons, L. K., Wang, Z., and Mak, J. E.: Joint application of concentration and δ18O to investigate the global atmospheric CO budget, Atmosphere, 6, 547–578, 2015.

Petrenko, M., Kahn, R., Chin, M., Soja, A., and Kucsera, T.: The use of satellite-measured aerosol optical depth to constrain biomass burning emissions source strength in the global model GOCART, J. Geophys. Res. Atmospheres, 117, 2012.

Pettinari, M. L. and Chuvieco, E.: Generation of a global fuel data set using the Fuel Characteristic Classification System, Biogeosciences, 13, 2061–2076, https://doi.org/10.5194/bg-13-2061-2016, 2016.

Potapov, P., Li, X., Hernandez-Serna, A., Tyukavina, A., Hansen, M. C., Kommareddy, A., Pickens, A., Turubanova, S., Tang, H., Silva, C. E., Armston, J., Dubayah, R., Blair, J. B., and Hofton, M.: Mapping global forest canopy height through integration of GEDI and Landsat data, Remote Sens. Environ., 253, 112165, https://doi.org/10.1016/j.rse.2020.112165, 2021.

Poulter, B., Frank, D., Ciais, P., Myneni, R. B., Andela, N., Bi, J., Broquet, G., Canadell, J. G., Chevallier, F., Liu, Y. Y., and others: Contribution of semi-arid ecosystems to interannual variability of the global carbon cycle, Nature, 509, 600–603, 2014.

Prichard, S. J., Kennedy, M. C., Andreu, A. G., Eagle, P. C., French, N. H., and Billmire, M.: Next-Generation Biomass Mapping for Regional Emissions and Carbon Inventories: Incorporating Uncertainty in Wildland Fuel Characterization, J. Geophys. Res. Biogeosciences, 124, 3699–3716, https://doi.org/10.1029/2019JG005083, 2019.

Quan, X., Yebra, M., Riaño, D., He, B., Lai, G., and Liu, X.: Global fuel moisture content mapping from MODIS, Int. J. Appl. Earth Obs. Geoinformation, 101, 102354, https://doi.org/10.1016/j.jag.2021.102354, 2021.

Quéré, C. L., Andrew, R. M., Friedlingstein, P., Sitch, S., Hauck, J., Pongratz, J., Pickers, P. A., Korsbakken, J. I., Peters, G. P., Canadell, J. G., Arneth, A., Arora, V. K., Barbero, L., Bastos, A., Bopp, L., Chevallier, F., Chini, L. P., Ciais, P., Doney, S. C., Gkritzalis, T., Goll, D. S., Harris, I., Haverd, V., Hoffman, F. M., Hoppema, M., Houghton, R. A., Hurtt, G., Ilyina, T., Jain, A. K., Johannessen, T., Jones, C. D., Kato, E., Keeling, R. F., Goldewijk, K. K., Landschützer, P., Lefèvre, N., Lienert, S., Liu, Z., Lombardozzi, D., Metzl, N., Munro, D. R., Nabel, J. E. M. S., Nakaoka, S., Neill, C., Olsen, A., Ono, T., Patra, P., Peregon, A., Peters, W., Peylin, P., Pfeil, B., Pierrot, D., Poulter, B., Rehder, G., Resplandy, L., Robertson, E., Rocher, M., Rödenbeck, C., Schuster, U., Schwinger, J., Séférian, R., Skjelvan, I., Steinhoff, T., Sutton, A., Tans, P. P., Tian, H., Tilbrook, B., Tubiello, F. N., Laan-Luijkx, I. T. van der, Werf, G. R. van der, Viovy, N., Walker, A. P., Wiltshire,

A. J., Wright, R., Zaehle, S., and Zheng, B.: Global Carbon Budget 2018, Earth Syst. Sci. Data, 10, 2141–2194, https://doi.org/10.5194/essd-10-2141-2018, 2018.

Ramo, R., Roteta, E., Bistinas, I., Wees, D. van, Bastarrika, A., Chuvieco, E., and Werf, G. R. van der: African burned area and fire carbon emissions are strongly impacted by small fires undetected by coarse resolution satellite data, Proc. Natl. Acad. Sci., 118, https://doi.org/10.1073/pnas.2011160118, 2021.

Rao, K., Williams, A. P., Flefil, J. F., and Konings, A. G.: SAR-enhanced mapping of live fuel moisture content, Remote Sens. Environ., 245, 111797, https://doi.org/10.1016/j.rse.2020.111797, 2020.

Rappaport, D. I., Morton, D. C., Longo, M., Keller, M., Dubayah, R., and dos-Santos, M. N.: Quantifying long-term changes in carbon stocks and forest structure from Amazon forest degradation, Environ. Res. Lett., 13, 065013, 2018.

Rémy, S., Veira, A., Paugam, R., Sofiev, M., Kaiser, J. W., Marenco, F., Burton, S. P., Benedetti, A., Engelen, R. J., Ferrare, R., and others: Two global data sets of daily fire emission injection heights since 2003, Atmospheric Chem. Phys., 17, 2921–2942, 2017.

Rémy, S., Kipling, Z., Huijnen, V., Flemming, J., Nabat, P., Michou, M., Ades, M., Engelen, R., and Peuch, V.-H.: Description and evaluation of the tropospheric aerosol scheme in the Integrated Forecasting System (IFS-AER, cycle 47R1) of ECMWF, Geosci. Model Dev. Discuss., 1–44, https://doi.org/10.5194/gmd-2021-264, 2021.

Rodríguez-Fernández, N. J., Mialon, A., Mermoz, S., Bouvet, A., Richaume, P., Bitar, A. A., Al-Yaari, A., Brandt, M., Kaminski, T., Toan, T. L., Kerr, Y. H., and Wigneron, J.-P.: An evaluation of SMOS L-band vegetation optical depth (L-VOD) data sets: high sensitivity of L-VOD to above-ground biomass in Africa, Biogeosciences, 15, 4627–4645, https://doi.org/10.5194/bg-15-4627-2018, 2018.

Roteta, E., Bastarrika, A., Padilla, M., Storm, T., and Chuvieco, E.: Development of a Sentinel-2 burned area algorithm: Generation of a small fire database for sub-Saharan Africa, Remote Sens. Environ., 222, 1–17, 2019.

Roy, D. P., Huang, H., Boschetti, L., Giglio, L., Yan, L., Zhang, H. H., and Li, Z.: Landsat-8 and Sentinel-2 burned area mapping - A combined sensor multi-temporal change detection approach, Remote Sens. Environ., 231, 111254, https://doi.org/10.1016/j.rse.2019.111254, 2019.

Saatchi, S. S., Harris, N. L., Brown, S., Lefsky, M., Mitchard, E. T. A., Salas, W., Zutta, B. R., Buermann, W., Lewis, S. L., Hagen, S., Petrova, S., White, L., Silman, M., and Morel, A.: Benchmark map of forest carbon stocks in tropical regions across three continents, Proc. Natl. Acad. Sci., 108, 9899–9904, https://doi.org/10.1073/pnas.1019576108, 2011.

Santoro, M., Cartus, O., Carvalhais, N., Rozendaal, D. M. A., Avitabile, V., Araza, A., de Bruin, S., Herold, M., Quegan, S., Rodríguez-Veiga, P., Balzter, H., Carreiras, J., Schepaschenko, D., Korets, M., Shimada, M., Itoh, T., Moreno Martínez, Á., Cavlovic, J., Cazzolla Gatti, R., da Conceição Bispo, P., Dewnath, N., Labrière, N., Liang, J., Lindsell, J., Mitchard, E. T. A., Morel, A., Pacheco Pascagaza, A. M., Ryan, C. M., Slik, F., Vaglio Laurin, G., Verbeeck, H., Wijaya, A., and Willcock, S.: The global forest above-ground biomass pool for 2010 estimated from high-resolution satellite observations, Earth Syst. Sci. Data, 13, 3927–3950, https://doi.org/10.5194/essd-13-3927-2021, 2021.

van der Schalie, R., de Jeu, R. A. M., Kerr, Y. H., Wigneron, J. P., Rodríguez-Fernández, N. J., Al-Yaari, A., Parinussa, R. M., Mecklenburg, S., and Drusch, M.: The merging of radiative transfer based surface soil moisture data from SMOS and AMSR-E, Remote Sens. Environ., 189, 180–193, https://doi.org/10.1016/j.rse.2016.11.026, 2017.

Schepaschenko, D., Chave, J., Phillips, O. L., Lewis, S. L., Davies, S. J., Réjou-Méchain, M., Sist, P., Scipal, K., Perger, C., Herault, B., Labrière, N., Hofhansl, F., Affum-Baffoe, K., Aleinikov, A., Alonso, A., Amani, C., Araujo-Murakami, A., Armston, J., Arroyo, L., Ascarrunz, N., Azevedo, C., Baker, T., Bałazy, R., Bedeau, C., Berry, N., Bilous, A. M., Bilous, S. Y., Bissiengou, P., Blanc, L., Bobkova, K. S., Braslavskaya, T., Brienen, R., Burslem, D. F. R. P., Condit, R., Cuni-Sanchez, A., Danilina, D., del Castillo Torres, D., Derroire, G., Descroix, L., Sotta, E. D., d'Oliveira, M. V. N., Dresel, C., Erwin, T., Evdokimenko, M. D., Falck, J., Feldpausch, T. R., Foli, E. G., Foster, R., Fritz, S., Garcia-Abril, A. D., Gornov, A., Gornova, M., Gothard-Bassébé, E., Gourlet-Fleury, S., Guedes, M., Hamer, K. C., Susanty, F. H., Higuchi, N., Coronado, E. N. H., Hubau, W., Hubbell, S., Ilstedt, U., Ivanov, V. V., Kanashiro, M., Karlsson, A., Karminov, V. N., Killeen, T., Koffi, J.-C. K., Konovalova, M., Kraxner, F., Krejza, J., Krisnawati, H., Krivobokov, L. V., Kuznetsov, M. A., Lakyda, I., Lakyda, P. I., Licona, J. C., Lucas, R. M., Lukina, N., Lussetti, D., Malhi, Y., Manzanera, J. A., Marimon, B., Junior, B. H. M., Martinez, R. V., Martynenko, O. V., Matsala, M., Matyashuk, R. K., Mazzei, L., Memiaghe, H., Mendoza, C., Mendoza, A. M., Moroziuk, O. V., Mukhortova, L., Musa, S., Nazimova, D. I., Okuda, T., Oliveira, L. C., Ontikov, P. V., et al.: The Forest Observation System, building a global reference dataset for remote sensing of forest biomass, Sci. Data, 6, 198, https://doi.org/10.1038/s41597-019-0196-1, 2019.

Seiler, W. and Crutzen, P. J.: Estimates of gross and net fluxes of carbon between the biosphere and the atmosphere from biomass burning, Clim. Change, 2, 207–247, https://doi.org/10.1007/BF00137988, 1980.

Shvetsov, E. G., Kukavskaya, E. A., Buryak, L. V., and Barrett, K.: Assessment of post-fire vegetation recovery in Southern Siberia using remote sensing observations, Environ. Res. Lett., 14, 055001, https://doi.org/10.1088/1748-9326/ab083d, 2019.

Simard, M., Pinto, N., Fisher, J. B., and Baccini, A.: Mapping forest canopy height globally with spaceborne lidar, J. Geophys. Res. Biogeosciences, 116, G04021, https://doi.org/10.1029/2011JG001708, 2011.

Thurner, M., Beer, C., Santoro, M., Carvalhais, N., Wutzler, T., Schepaschenko, D., Shvidenko, A., Kompter, E., Ahrens, B., Levick, S. R., and Schmullius, C.: Carbon stock and density of northern boreal and temperate forests, Glob. Ecol. Biogeogr., 23, 297–310, https://doi.org/10.1111/geb.12125, 2014.

Torres, O., Jethva, H., Ahn, C., Jaross, G., and Loyola, D. G.: TROPOMI Aerosol Products: Evaluation and Observations of Synoptic Scale Carbonaceous Aerosol Plumes during 2018–2020, Atmospheric Meas. Tech. Discuss., 1–20, https://doi.org/10.5194/amt-2020-124, 2020.

Veefkind, J. P., Aben, I., McMullan, K., Förster, H., de Vries, J., Otter, G., Claas, J., Eskes, H. J., de Haan, J. F., Kleipool, Q., van Weele, M., Hasekamp, O., Hoogeveen, R., Landgraf, J., Snel, R., Tol, P., Ingmann, P., Voors, R., Kruizinga, B., Vink, R., Visser, H., and Levelt, P. F.: TROPOMI on the ESA Sentinel-5 Precursor: A GMES mission for global observations of the atmospheric composition for climate, air quality and ozone layer applications, Remote Sens. Environ., 120, 70–83, https://doi.org/10.1016/j.rse.2011.09.027, 2012.

van der Velde, I. R., van der Werf, G. R., Houweling, S., Maasakkers, J. D., Borsdorff, T., Landgraf, J., Tol, P., van Kempen, T. A., van Hees, R., Hoogeveen, R., Veefkind, J. P., and Aben, I.: Vast CO_2 release from Australian fires in 2019–2020 constrained by satellite, Nature, 597, 366–369, https://doi.org/10.1038/s41586-021-03712-y, 2021.

Veraverbeke, S., Sedano, F., Hook, S. J., Randerson, J. T., Jin, Y., and Rogers, B. M.: Mapping the daily progression of large wildland fires using MODIS active fire data, Int. J. Wildland Fire, 23, 655–667, 2014.

Vigouroux, C., Langerock, B., Bauer Aquino, C. A., Blumenstock, T., Cheng, Z., De Mazière, M., De Smedt, I., Grutter, M., Hannigan, J. W., Jones, N., Kivi, R., Loyola, D., Lutsch, E., Mahieu, E., Makarova, M., Metzger, J.-M., Morino, I., Murata, I., Nagahama, T., Notholt, J., Ortega, I., Palm, M., Pinardi, G., Röhling, A., Smale, D., Stremme, W., Strong, K., Sussmann, R., Té, Y., van Roozendael, M., Wang, P., and Winkler, H.: TROPOMI–Sentinel-5 Precursor formaldehyde validation using an extensive network of ground-based Fourier-transform infrared stations, Atmospheric Meas. Tech., 13, 3751–3767, https://doi.org/10.5194/amt-13-3751-2020, 2020.

Vittucci, C., Vaglio Laurin, G., Tramontana, G., Ferrazzoli, P., Guerriero, L., and Papale, D.: Vegetation optical depth at L-band and above ground biomass in the tropical range: Evaluating their relationships at continental and regional scales, Int. J. Appl. Earth Obs. Geoinformation, 77, 151–161, https://doi.org/10.1016/j.jag.2019.01.006, 2019.

Walker, X. J., Rogers, B. M., Veraverbeke, S., Johnstone, J. F., Baltzer, J. L., Barrett, K., Bourgeau-Chavez, L., Day, N. J., de Groot, W. J., Dieleman, C. M., Goetz, S., Hoy, E., Jenkins, L. K., Kane, E. S., Parisien, M.-A., Potter, S., Schuur, E. a. G., Turetsky, M., Whitman, E., and Mack, M. C.: Fuel availability not fire weather controls boreal wildfire severity and carbon emissions, Nat. Clim. Change, 10, 1130–1136, https://doi.org/10.1038/s41558-020-00920-8, 2020.

Ward, D. S., Kloster, S., Mahowald, N. M., Rogers, B. M., Randerson, J. T., and Hess, P. G.: The changing radiative forcing of fires: global model estimates for past, present and future, Atmos Chem Phys, 12, 10857–10886, https://doi.org/10.5194/acp-12-10857-2012, 2012.

Weidong, X., Wooster, M. J., He, J., and Zhang, T.: First study of Sentinel-3 SLSTR active fire detection and FRP retrieval: Night-time algorithm enhancements and global intercomparison to MODIS and VIIRS AF products, Remote Sens. Environ., 248, 111947, 2020.

van der Werf, G. R., Randerson, J. T., Collatz, G. J., Giglio, L., Kasibhatla, P. S., Arellano, A. F., Olsen, S. C., and Kasischke, E. S.: Continental-scale partitioning of fire emissions during the 1997 to 2001 El Nino/La Nina period, Science, 303, 73–76, 2004.

van der Werf, G. R., Randerson, J. T., Giglio, L., Collatz, G. J., Kasibhatla, P. S., and Arellano Jr, A. F.: Interannual variability in global biomass burning emissions from 1997 to 2004, Atmospheric Chem. Phys., 6, 3423–3441, 2006.

van der Werf, G. R., Randerson, J. T., Giglio, L., Van Leeuwen, T. T., Chen, Y., Rogers, B. M., Mu, M., Van Marle, M. J., Morton, D. C., Collatz, G. J., and others: Global fire emissions estimates during 1997-2016, Earth Syst. Sci. Data, 9, 697–720, 2017.

Wigneron, J.-P., Li, X., Frappart, F., Fan, L., Al-Yaari, A., De Lannoy, G., Liu, X., Wang, M., Le Masson, E., and Moisy, C.: SMOS-IC data record of soil moisture and L-VOD: Historical development, applications and perspectives, Remote Sens. Environ., 254, 112238, https://doi.org/10.1016/j.rse.2020.112238, 2021.

Williams, J. E., Huijnen, V., Bouarar, I., Meziane, M., Schreurs, T., Pelletier, S., Marécal, V., Josse, B., and Flemming, J.: Regional evaluation of the performance of the global CAMS chemical modeling system over the United States (IFS cycle 47r1), Geosci. Model Dev. Discuss., 1–39, https://doi.org/10.5194/gmd-2021-318, 2021.

Williamson, G. J., Prior, L. D., Jolly, W. M., Cochrane, M. A., Murphy, B. P., and Bowman, D. M. J. S.: Measurement of inter- and intra-annual variability of landscape fire activity at a continental scale: the Australian case, Environ. Res. Lett., 11, 035003, https://doi.org/10.1088/1748-9326/11/3/035003, 2016.

Wooster, M. J., Roberts, G., Perry, G. L. W., and Kaufman, Y. J.: Retrieval of biomass combustion rates and totals from fire radiative power observations: FRP derivation and calibration

relationships between biomass consumption and fire radiative energy release, J. Geophys. Res. Atmospheres, 110, D24311, https://doi.org/10.1029/2005JD006318, 2005.

Yebra, M., Dennison, P. E., Chuvieco, E., Riaño, D., Zylstra, P., Hunt Jr., E. R., Danson, F. M., Qi, Y., and Jurdao, S.: A global review of remote sensing of live fuel moisture content for fire danger assessment: Moving towards operational products, Remote Sens. Environ., 136, 455–468, https://doi.org/10.1016/j.rse.2013.05.029, 2013.

Yebra, M., Quan, X., Riaño, D., Rozas Larraondo, P., van Dijk, A. I. J. M., and Cary, G. J.: A fuel moisture content and flammability monitoring methodology for continental Australia based on optical remote sensing, Remote Sens. Environ., 212, 260–272, https://doi.org/10.1016/j.rse.2018.04.053, 2018.

Yebra, M., Scortechini, G., Badi, A., Beget, M. E., Boer, M. M., Bradstock, R., Chuvieco, E., Danson, F. M., Dennison, P., Dios, V. R. de, Bella, C. M. D., Forsyth, G., Frost, P., Garcia, M., Hamdi, A., He, B., Jolly, M., Kraaij, T., Martín, M. P., Mouillot, F., Newnham, G., Nolan, R. H., Pellizzaro, G., Qi, Y., Quan, X., Riaño, D., Roberts, D., Sow, M., and Ustin, S.: Globe-LFMC, a global plant water status database for vegetation ecophysiology and wildfire applications, Sci. Data, 6, 1–8, https://doi.org/10.1038/s41597-019-0164-9, 2019.

Zhang, H., Hagan, D. F. T., Dalagnol, R., and Liu, Y.: Forest Canopy Changes in the Southern Amazon during the 2019 Fire Season Based on Passive Microwave and Optical Satellite Observations, Remote Sens., 13, 2238, https://doi.org/10.3390/rs13122238, 2021.